Metrologia **51** (2014) *Tech. Suppl.* 06019

Key Comparison APMP.RI(I)-K2 of air kerma standards for the CCRI reference radiation qualities for low-energy x-rays, including a supplementary comparison for the ISO 4037 narrow spectrum series

T. Tanaka[f], N. Saito[f], M. Bero[a], D. Butler[b], A.K. Mahant[c], A. Meghzifene[d], C.H. Chu[e], T.B. Kadni[g], WU. Jinjie[h], T. Soodprasert[i]

[a] *Atomic Energy Commission, Damascus, Syria*

[b] *Australian Radiation Protection and Nuclear Safety Agency, Yallambie, Australia*

[c] *Bhabha Atomic Research Centre, Mumbai, India*

[d] *International Atomic Energy Agency, Vienna*

[e] *Institute of Nuclear Energy Research, Longtan, Taiwan*

[f] *National Metrology Institute of Japan, Tsukuba, Japan*

[g] *Malaysian Nuclear Agency (Nuclear Malaysia), Kajang, Malaysia*

[h] *National Institute of Metrology, Beijing, China*

[i] *Office of Atoms for Peace, Bangkok, Thailand*

Abstract

An indirect comparison was performed between nine national[1] standards for air kerma for the CCRI radiation qualities from 10 kV to 50 kV (APMP.RI(I)-K2) and for the ISO 4037 narrow spectrum series (15 kV and 40 kV). Among the nine institutes that participated in the comparison, seven institutes were APMP member laboratories. Three commercially available thin window parallel plate ionization chambers were used as transfer instruments and circulated among the participants. The pilot laboratory, the NMIJ/AIST, served also as the link to the corresponding BIPM.RI(I)-K2 comparison. The results show general agreement within the combined uncertainties, although certain results for Nuclear Malaysia, the BARC and the OAP show larger differences.

1. Introduction

An indirect comparison has been made between the air kerma standards of the participating national metrological institutes (NMIs) for the CCRI reference radiation qualities from 10 kV to 50 kV [1], and for the ISO 4037 narrow spectrum series (15 kV and 40 kV) [2]. The object of this key comparison is to establish the degree of equivalence between the participating NMIs, and to support the mutual recognition of calibration certificates for these radiation qualities. Three transfer

[1] To simplify the text, the IAEA and its secondary standard, traceable to the BIPM, are grouped with the national laboratories and standards in the present report.

chambers of different types were calibrated by each participating laboratory for these radiation qualities.

2. Procedure

2.1 Transfer chambers

Table 1 shows the characteristics of the three cavity chambers used as the transfer chambers for the comparison. These chambers are provided by the NMIJ/AIST (the Magna and AE-1340C chambers) and the ARPANSA (the NE 2536 chamber). The reference plane for each chamber is the front surface of the chamber. The signal connections for the chambers are a tri-axial plug for the Magna and NE 2536 chambers and a BNC with a 4 mm 'banana' plug for the AE-1340C chamber. Photographs of the transfer chambers are shown in Appendix A. An ambiguity in how the stated polarizing potential is applied (to the collector or to the window) is discussed later.

Table 1. Technical data of the transfer chambers

Supplier	Model	Serial Number	Nominal volume	Entrance window	Polarizing potential	Cable connection
EXRADIN	Magna	D070313	3 cm^3	3.86 mg cm^{-2}	-250 V	Tri-axial (BNT)
OYOGIKEN	AE-1340C	1042	0.24 cm^3	50 μm PET	-250 V	Signal: BNC HV: banana plug
NE	2536/3	R17804	0.3 cm^3	2.3 mg cm^{-2}	-250 V	Tri-axial (BNT) or Tri-axial (TNC)

2.2 Radiation qualities and reference conditions

The radiation qualities used for the comparison were the CCRI reference qualities for the low-energy x-ray range (10 kV, 30 kV, 25 kV, 50 kV(b), 50 kV(a)) [1] and the narrow-spectrum series defined in ISO 4037-1 (15 kV and 40 kV) [2]. The characteristics of these radiation qualities are shown in Table 2; for the CCRI qualities the values shown are for the BIPM realizations, while for the ISO qualities the values are nominal.

Table 2. Characteristics of CCRI reference qualities and ISO 4037 narrow spectrum series

Reference	CCRI					ISO 4037 narrow	
X-ray tube voltage /kV	10	30	25	50b	50a	15	40
Additional filtration							
mm Al	0	0.208	0.372	1.008	3.989	0.1	4.0
mm Cu	-	-	-	-	-	-	0.21
1st Half-value layer							
mmAl	0.037	0.169	0.242	1.017	2.262	0.14	-
mmCu	-	-	-	-	-	-	0.084
2nd Half-value layer							
mmAl	-	-	-	-	-	0.16	-
mmCu	-	-	-	-	-	-	0.091

The reference conditions for the chamber calibrations were as follows:

1. Distance from the focal spot to the reference plane (the front surface of the chamber): 1.0 m
2. Field size at the reference plane: 10 cm in diameter
3. Air temperature, pressure and relative humidity: T = 293.15 K, P = 1013.25 hPa and h = 50 %
4. The calibration coefficients for the transfer chambers should be given in terms of air kerma per charge, in units of Gy C^{-1}.

2.3 Participants and course of comparison

Nine institutes listed in Table 3 participated in the comparison. The NMIJ/AIST was both the pilot laboratory and the linking laboratory. The ARPANSA could also have been a linking laboratory. As described below, however, the calibration distance at the ARPANSA is different from that at the other participating institutes. Therefore only the NMIJ was treated as a linking laboratory to avoid introducing additional uncertainty associated with this difference.

Table 3. Participating Institutes

Institute		Country
AEC	Atomic Energy Commission	Syria
ARPANSA	Australian Radiation Protection and Nuclear Safety Agency	Australia
BARC	Bhabha Atomic Research Centre	India
IAEA	International Atomic Energy Agency	IAEA
INER	Institute of Nuclear Energy Research	Taiwan
NMIJ/AIST	National Metrology Institute of Japan, National Institute of Advanced Industrial Science and Technology	Japan
Nuclear Malaysia	Malaysian Nuclear Agency	Malaysia
NIM	National Institute of Metrology	China
OAP	Office of Atoms for Peace	Thailand

A star-shaped circulation of the chambers between NMIJ/AIST and the other participants was realized. After each participant's calibration the NMIJ/AIST checked the chamber constancy (except after measurements at the ARPANSA and the AEC when the chambers were sent directly to the next laboratory). The chambers stayed with each participant for no longer than 3 weeks. The results were reported to the pilot laboratory within 6 weeks of each calibration. An MS-Excel sheet was provided by the pilot laboratory in which information on the participants' radiation qualities, primary standards and calibration results were completed. All participants were required to evaluate the uncertainty of their calibration coefficients as Type A and Type B according to the criteria given in the "Guide to The Expression of Uncertainty in Measurement" issued by the International Organization for Standardization (ISO) in 1995 [3]. The Type A uncertainty is obtained by the statistical analysis of a series of observations; the Type B uncertainty is obtained by means other than the statistical analysis of series of observations. In order to analyse the uncertainties and to take

correlation into account for degrees of equivalence entered in the BIPM key comparison database [4], the CIPM requires that the participating laboratories submit their detailed uncertainty budgets (with relative standard uncertainties, $k = 1$) to the pilot laboratory. An MS-Excel sheet was provided by the pilot laboratory in which the participants could detail the uncertainty. The sheet was submitted together with the calibration results. The comparison was conducted from August 2008 until May 2011, as shown in Table 4.

Table 4. Date of calibration at the participants and constancy check at NMIJ/AIST

Participant	Date of calibration	Constancy check
NMIJ/AIST	Aug-2008	
Nuc. Malaysia	Sep-2008	Oct-2008
BARC	Feb-2009	Dec-2008 and Mar-2009
ARPANSA	Apr-2009	N.A. *
INER	Aug-2009	Aug-2009
OAP	Dec-2009	Oct-2009 and Feb-2010
AEC	Apr-2010	N.A.**
IAEA	Jul-2010	Aug-2010
NIM	Nov-2010	Oct-2010 and May-2011

* the NMIJ/AIST x-ray facility was temporarily unavailable.
** direct transport from AEC to IAEA

3. The linking of regional comparisons to international comparisons

To link the APMP comparison (a regional comparison) with the BIPM (an international comparison), the NMIJ/AIST, which had made a key comparison with the BIPM for air kerma in low-energy x-rays, was used as a "linking laboratory". The calibration coefficients measured at each laboratory were converted to ratios relative to the BIPM using the equation:

$$R_{\mathrm{NMI,BIPM}} = R_{\mathrm{NMI,Link}} \times R_{\mathrm{Link,BIPM}} \qquad (1)$$

In this equation,

$R_{\mathrm{NMI,BIPM}}$ = the derived ratio of air kerma determinations of the participating NMI and the BIPM for the quality.

$R_{\mathrm{NMI,Link}}$ = the ratio of the air kerma determinations of a participating NMI and the linking laboratory, which is represented numerically by the corresponding mean ratio of the calibration coefficients from the present comparison at a given radiation quality

$R_{\mathrm{Link,BIPM}}$ = the ratio of the air kerma determinations of the linking laboratory and the BIPM obtained for the corresponding quality in the BIPM.RI(I)-K2 key comparison

The NMIJ/AIST made a bilateral comparison with the BIPM in 2004 [5], for which the measured values of the NMIJ/AIST and BIPM calibration coefficients agreed within 0.6 % for the CCRI reference qualities. The comparison results between the NMIJ/AIST and the BIPM for low-energy x-rays used as the links $R_{\mathrm{Link,BIPM}}$ are given in Table 5.

Table 5. Key comparison ratios NMI/BIPM for the CCRI radiation qulities for the NMIJ.

Laboratory	Year	X-ray tube voltage / kV					Combined standard uncertainties
		10	30	25	50b	50a	
NMIJ/AIST	2004	1.0009	1.0010	1.0032	1.0046	1.0054	0.18 %

4. Results

4.1 Energy dependence of the calibration coefficient of the transfer chambers

The calibration coefficients of the three ionization chambers measured at the NMIJ/AIST are shown in Figure 1. They are normalized to the values for the CCRI 50b radiation quality. The AE-1340C chamber shows a flat energy dependence at the 1 % level in the range of aluminium half-value layers (HVLs) from 0.15 mm to 3 mm. On the other hand, the calibration coefficient for the chamber increases significantly below this range. The calibration coefficient of the NE2536 chamber decreases with the increase of HVL at an approximately constant rate with HVL when plotted on a logarithmic scale. The energy dependence of the Magna chamber is similar to that of the NE2536 chamber except for the CCRI-10 radiation quality.

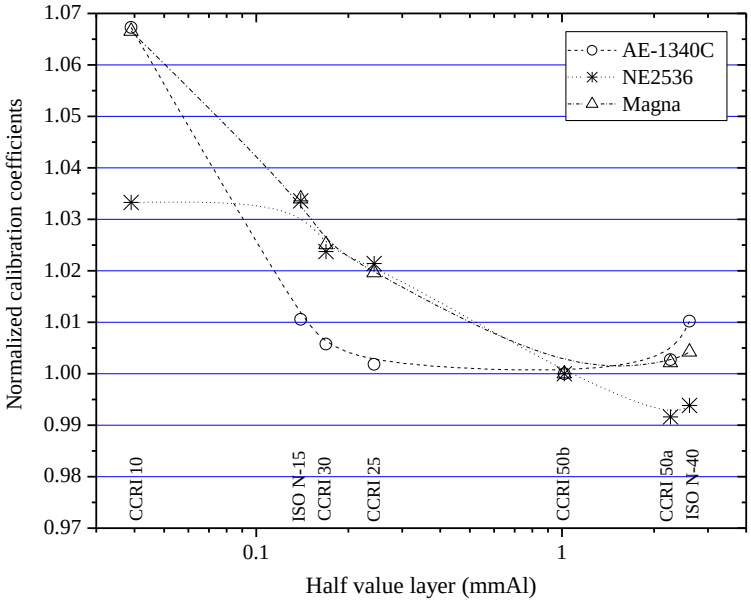

Figure 1. Calibration coefficients normalized to those for the CCRI 50b radiation quality. The uncertainty bars of 0.6 % (k = 1) are not shown.

4.2 Stability measurements

Stability measurements were performed at the NMIJ/AIST after each participant's measurements, except after returning from the ARPANSA when the NMIJ/AIST x-ray facility was temporarily unavailable (see also Table 4). All transfer chambers were calibrated for all of the CCRI reference

qualities and for the ISO 4037 N-15 and N-40 qualities. The mean values and relative standard deviations of calibration coefficients are shown in Table 6. The normalized calibration coefficients of the transfer chambers measured during the comparison period are shown in Figs. 2, 3 and 4.

Table 6. Mean values and relative standard deviations of the calibration coefficients measured at the NMIJ/AIST during the star shaped comparison

	Magna		AE-1340C		NE2536 (bef. Feb-10)		NE2536 (after Aug-10)	
	Mean N_K	S-Dev	Mean N_K	S-Dev	Mean N_K	S-Dev	Mean N_K	S-Dev
	10^7 Gy/C	%	10^8 Gy/C	%	10^8 Gy/C	%	10^8 Gy/C	%
CCRI 10	0.8845	0.14	1.1709	0.12	0.9226	0.12	0.9079	0.14
CCRI 30	0.8501	0.08	1.1034	0.10	0.9141	0.03	0.9007	0.03
CCRI 25	0.8456	0.09	1.0991	0.07	0.9120	0.07	0.8984	0.13
CCRI 50b	0.8293	0.10	1.0971	0.10	0.8929	0.06	0.8786	0.07
CCRI 50a	0.8311	0.11	1.1001	0.07	0.8854	0.08	0.8705	0.03
mean (u_{stab})		0.11		0.09		0.07		0.08
ISO N-15	0.8575	0.13	1.1087	0.14	0.9229	0.09	0.9078	0.11
ISO N-40	0.8328	0.22	1.1083	0.36	0.8874	0.19	0.8738	0.31

As shown in Figure 4a, the NE2536 chamber calibration coefficients changed by about 1.5 % for all of the radiation qualities after returning from the IAEA *i.e.* from the consistency check in August 2010 onwards. A tiny defect was observed on the front surface of the chamber as shown in the photographs in Appendix B. This defect is suspected of being the cause of the change in calibration coefficients. It was not possible to know when the calibration coefficients changed, because the chamber was transported from the AEC to the IAEA directly. The mean values of the calibration coefficients of the NE2536 chamber were calculated separately for the two periods; (i) before sending them to the AEC, (ii) after their return from the IAEA. The results shown in Figure 4b were obtained by re-normalization to the mean values obtained for the two periods separately.

From the results shown in Figs. 2, 3 and 4b, it can be concluded that the chambers were sufficiently stable through the comparison period. The uncertainty u_{stab} associated with the long-term stability of the transfer chambers are evaluated as mean values for the CCRI radiation qualities, where u_{stab} = 0.11 % for the Magna, 0.09 % for the AE-1340 and 0.08 % for the NE2536. The relative standard deviations of the calibration coefficients of all of the transfer chambers for the ISO N-40 radiation are relatively high compared to the values for the other radiation qualities. The air kerma rates of the ISO N-40 radiation were of the order of tens of μGy/s (see Table 7b), which is lower by two orders of magnitude than those for the other radiation qualities. The low air kerma rates are assumed to be responsible for the higher type A uncertainties.

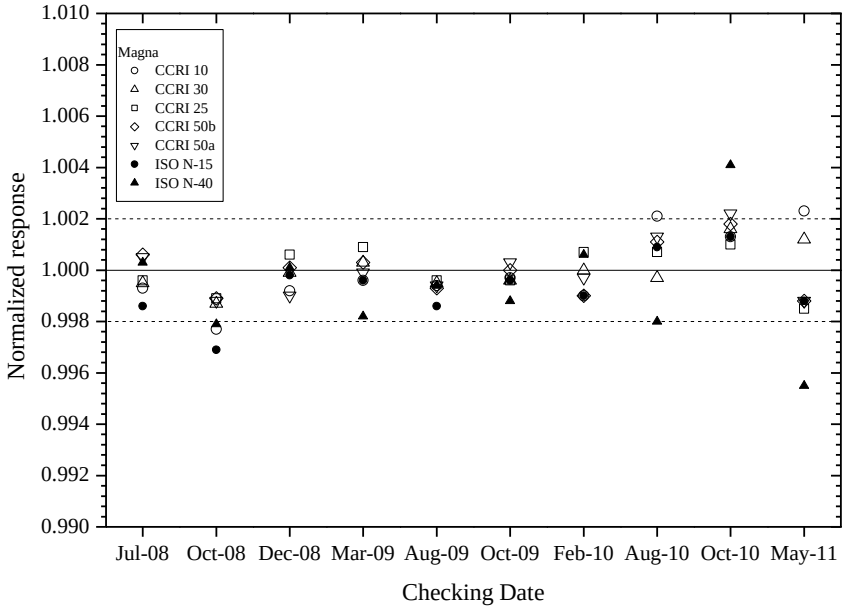

Figure 2. Stability of the Magna transfer chamber.

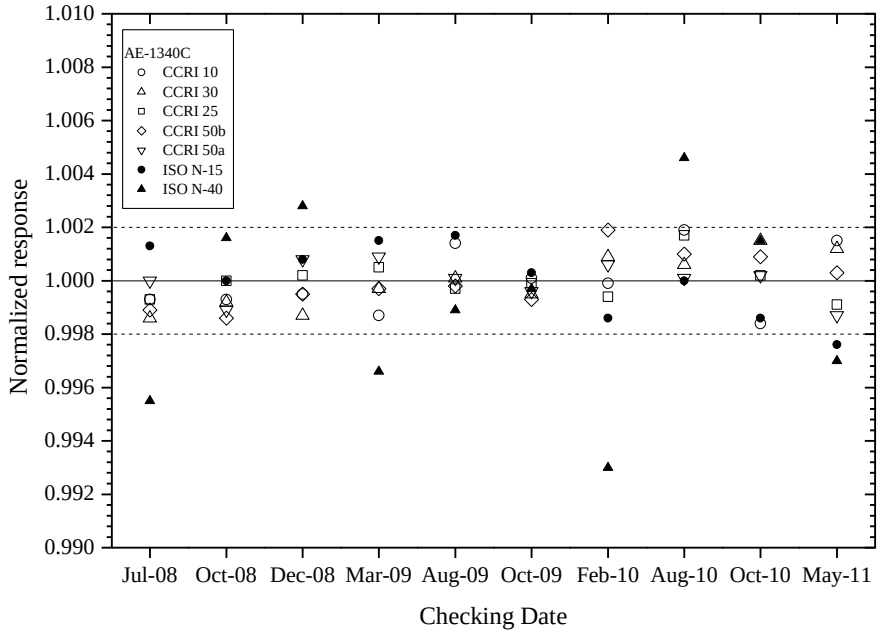

Figure 3. Stability of the AE-1340C transfer chamber.

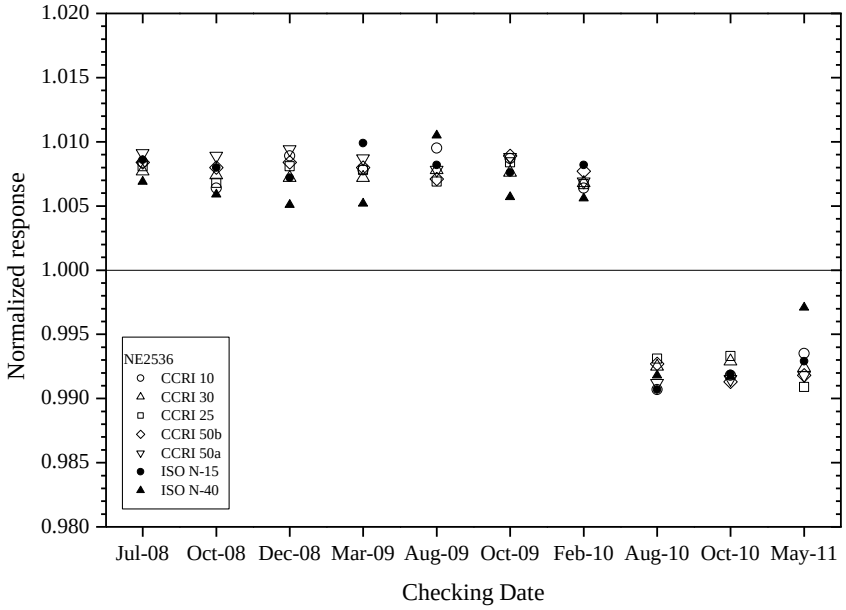

Figure 4a. Stability of the NE2536 transfer chamber.

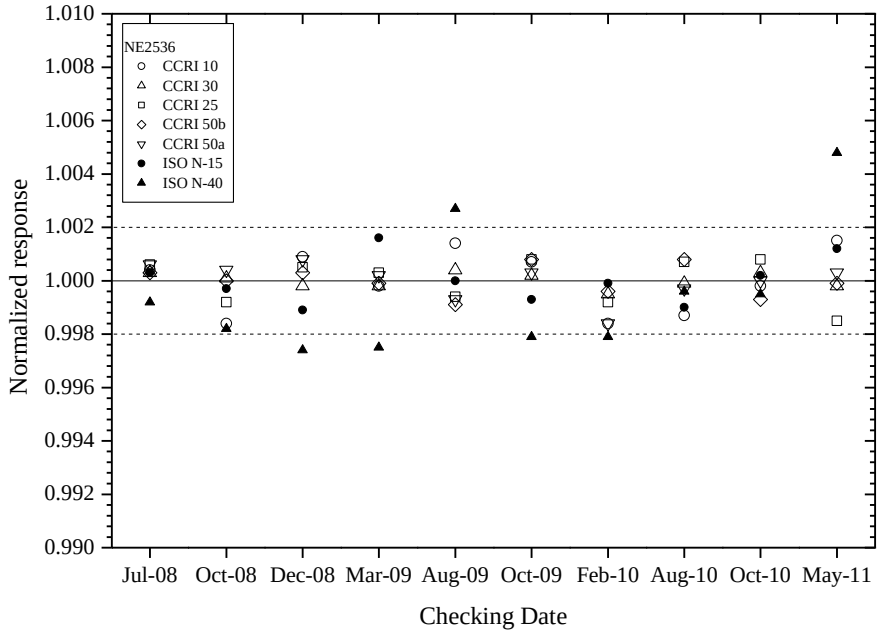

Figure 4b. Stability of the NE2536 transfer chamber after re-normalization separately for those measured from August 2010 onwards.

4.3 National air kerma standards and calibration conditions

The technical data of the national air kerma standards and parameters characterizing the calibration conditions at the participant institutes are summarized in Tables 7a and 7b. The AEC, IAEA, Nuclear Malaysia and OAP do not have primary standards and use secondary standard ionization chambers, which are traceable to the primary standard laboratories indicated in the table. The INER used a cylindrical parallel type free air chamber (FAC) and the other primary standard laboratories used plane parallel type FACs.

Table 7a. Technical data of the national air kerma standards

Participants	Chamber type	Standard traceability	Aperture diameter	Collecting length	Electrode separation	Collector width	Measuring volume	Attenuation length	Polarizing voltage
AEC	PTW 23342	BIPM via IAEA	-	-	-	-	0.02 cm^3	-	300 V
ARPANSA	plane parallel FAC	ARPANSA	0.50 cm	2.00 cm	6.00 cm	8.00 cm	0.39465 cm^3	8.50 cm	-3000 V
BARC	plane parallel FAC	BARC	1.0 cm	10.0 cm	28.0 cm	38.2 cm	7.854 cm^3	34.3 cm	1000 to 2000V
IAEA	PTW 23344	BIPM	-	-	-	-	0.2 cm^3	-	-
INER	cylindric FAC	INER	0.4 cm	7 cm	8.00 cm	-	0.855 cm^3	15.5 cm	1500 V
NMIJ/AIST	plane parallel FAC	NMIJ/AIST	0.6024 cm	2.026 cm	7.99 cm	8.044 cm	0.577 cm^3	8.00 cm	2500 V
Nuc. Malaysia	PTW 23344	PTB	-	-	-	-	0.2 cm^3	-	300 V
NIM	plane parallel FAC	NIM	1.0022 cm	4.050 cm	7.92 cm	9.990 cm	3.194 cm^3	10.0 cm	1600 V
OAP	NE 2575	NPL	-	6.8 cm	-	-	600 cm^3	-	-300 V

Table 7b. Parameters characterizing the calibration conditions

Participants	Calibration distance (mm)	Field size (mm in dia.)	Air kerma rate (mGy/s)						
			CCRI 10	CCRI 30	CCRI 25	CCRI 50b	CCRI 50a	ISO N-15	ISO N-40
AEC	1000	100	-	6.03	2.15	2.51	0.46	-	-
ARPANSA	500	100	0.90	6.80	1.80	3.80	0.80	-	-
BARC	1000	100	-	3.85	1.37	2.05	0.42	0.05	0.05
IAEA	1000	100	0.77	0.98	1.40	0.92	0.59	-	-
INER	1000	100	0.13	1.72	0.65	0.91	0.19	0.21	0.04
NMIJ/AIST	1000	100	0.51	4.70	1.36	1.80	0.44	0.15	0.05
Nucl. Malaysia	1000	100	0.34	2.90	0.93	1.29	0.33	0.05	0.02
NIM	1000	120	0.52	3.00	3.00	3.10	0.52	0.52	0.08
OAP	1000	260	0.09	0.49	0.16	0.25	0.06	0.01	0.03

The air kerma rates for each radiation quality show variations by a factor of more than 10 for the different participants. The air kerma rates at the OAP are particularly low and their field size is very large; these choices result from their use of a large volume (600 cm^3) reference chamber. To obtain information on the effect of ion recombination on the calibration coefficients, additional measurements were performed at the NMIJ/AIST. The results of the air kerma rate dependence of the calibration coefficient for each transfer chamber are summarized in Table 8.

Table 8. Air kerma rate dependence of the calibration coefficients for each chamber.

air kerma rate	ratio of N_k relative to air kerma rate of 1.2 mGy/s		
(mGy/s)	Magna	AE-1340C	NE2536
0.1	0.9993	-	-
0.2	1.0001	1.0031	0.9992
0.6	1.0003	1.0010	0.9998
1.2	1.0000	1.0000	1.0000
3.5	1.0000	0.9983	1.0007
7.1*	1.0006	0.9974	1.0011

* for Magna, air kerma rate is 6.6 mGy/s

As can be seen from Table 8, the Magna and NE2536 chambers do not show an air kerma rate dependence of more than 0.1 % over the range from 0.2 mGy/s to 7.1 mGy/s. The calibration coefficient for the AE-1340C chamber, on the other hand, changed by 0.6 % over this range, decreasing for the higher air kerma rates in contrast to the increase that would be expected if ion recombination was responsible. The reason for this change is not known. Nevertheless, a correction factor for the AE-1340C chamber was evaluated by interpolation of the results and was applied when it exceeded 0.1 %. The uncertainty associated with the air kerma rate dependence is taken to be 0.1 % for the CCRI radiation qualities. For the ISO radiation qualities, on the other hand, no corresponding correction factor was applied because the air kerma rate was too low to obtain a reliable measurement of the effect. For these qualities, an uncertainty of 0.2 % is introduced for this effect.

The calibration distance was 500 mm at the ARPANSA and 1000 mm at all other participants. The report of the key comparison between the BIPM and the NRC for low energy x-rays suggests that the effect of calibration distance and field size on calibration coefficients might be over 1 % [6]. This is significantly larger than the statistical standard uncertainty of each calibration coefficient. In order to assess this effect quantitatively, the NMIJ/AIST performed additional measurements at a distance of 520 mm for all transfer chambers.

Table 9 shows the calibration coefficients of each transfer chamber measured at 520 mm. The ratios of the calibration coefficients measured at 520 mm to those measured at 1000 mm are also listed in the table. The ratios increase with the decrease of x-ray energy. The increases in the ratios are larger than the statistical standard uncertainty of each calibration coefficient in every case. The increase is quite large for the CCRI 10 radiation quality. This is due to the difference in the HVLs between 520 mm and 1000 mm (see also in Tables 12a and b). The large difference between the calibration coefficients measured at 520 mm and 1000 mm for the CCRI 10 radiation quality reflects the difference in the energy dependence of the chambers. Consequently, in the analysis that follows the ARPANSA results were compared to the NMIJ/AIST results measured at the calibration distance of 520 mm, not those measured at 1000 mm.

Table 9. The calibration coefficients measured at the calibration distance of 520 mm at the NIMJ/AIST.

	Magna			AE-1340C			NE2536 (bef. Feb-10)		
	N_K (520 mm)	relative standard uncertainty	ratio of N_k at 520 mm to N_k at 1000 mm	N_K (520 mm)	relative standard uncertainty	ratio of N_k at 520 mm to N_k at 1000 mm	N_K (520 mm)	relative standard uncertainty	ratio of N_k at 520 mm to N_k at 1000 mm
	10^7 Gy/C	%		10^8 Gy/C	%		10^8 Gy/C	%	
CCRI 10	0.9077	0.40	1.0262	1.2078	0.40	1.0315	0.9313	0.40	1.0094
CCRI 30	0.8598	0.40	1.0114	1.1127	0.40	1.0084	0.9214	0.40	1.0080
CCRI 25	0.8526	0.40	1.0083	1.1060	0.40	1.0063	0.9174	0.40	1.0059
CCRI 50b	0.8384	0.40	1.0110	1.1049	0.40	1.0071	0.8991	0.40	1.0069
CCRI 50a	0.8405	0.40	1.0112	1.1062	0.40	1.0056	0.8934	0.40	1.0090

Subsequent to the comparison measurements, it was realized that the instructions for applying the polarity in the technical protocol of the present comparison could be interpreted in different ways. To clear up any ambiguity the NMIJ/AIST asked the participants about the applied voltages and collected charge polarity. The answers are summarized in Table 10.

Table 10. Applied voltages to each transfer chamber and collected charge polarity

	Magna				AE-1340C				NE2536			
Participant	Collected charge polarity	Potential (V) Triaxial center	Triaxial middle	Triaxial outer	Collected charge polarity	Potential (V) BNC center	BNC outer	banana connector	Collected charge polarity	Potential (V) Triaxial center	Triaxial middle	Triaxial outer
AEC	-	-	-	-	negative	250	250	GND	negative	250	250	GND
ARPANSA	negative	GND	GND	-250	negative	GND	GND	-250	negative	GND	GND	-250
BARC	-	-	-	-	-	-	-	-	-	-	-	-
IAEA	negative	250	250	GND	negative	GND	GND	-250	negative	250	250	GND
INER	positive	-	-	-	positive	-	-	-	positive	-	-	-
NMIJ/AIST	negative	GND	GND	-250	negative	GND	GND	-250	negative	GND	GND	-250
Nuc. Malaysia	-	-	-	-	-	-	-	-	-	-	-	-
NIM	negative	GND	GND	-250	negative	GND	GND	-250	negative	GND	GND	-250
OAP	negative	-	-250	GND	negative	-	-250	GND	negative	-	-250	GND

Most participants applied either:

(i) a negative potential to the chamber window, with the collector at a ground potential,

(ii) a positive potential to the collector, with the chamber window at a ground potential.

In both cases, negative charge was collected and no corrections are applied for polarity effects. The OAP used a different arrangement but also measured negative charge. On the other hand, positive charge was collected at the INER. The NMIJ/AIST performed additional measurements to check the polarity effects for each chamber and the results are presented in Table 11.

Table 11. Polarity effects on the calibration coefficients for each chamber.

	-250/+250 (ratio of N_k)		
	Magna	AE-1340C	NE2536
CCRI 10	0.9976	0.9968	0.9982
CCRI 30	1.0006	0.9961	1.0010
CCRI 25	1.0011	0.9978	1.0024
CCRI 50b	1.0008	0.9975	1.0004
CCRI 50a	1.0017	0.9986	1.0002
Mean	1.0004	0.9974	1.0004

For the Magna and NE2536 chambers the polarity effects are negligible (the variations seen at the different qualities are assumed to be statistical). The AE-1340C chamber, on the other hand, shows a polarity effect of about 0.3 % with perhaps some energy dependence. Considering the statistical uncertainty of each calibration coefficient of about 0.1 %, however, the best estimate of the polarity effect for the AE-1340C chamber was taken to be the mean value. In the following analysis, this polarity correction factor is applied to the AE-1340C chamber calibration coefficients for all of the radiation qualities at the INER.

The HVLs for the CCRI reference radiation qualities and ISO 4037 narrow spectrum series realized

at the participant's sites are listed in Table 12a together with the reference values given in Reference [1] and [2]. It is noted that these reference values are for a distance of 500 mm, not 1000 mm, which can have a significant effect at 10 kV. However, for the purpose of normalization, the use of the reference values at 500 mm is sufficient.

Table 12b shows the HVLs normalized to each reference value. The differences in the HVL of the CCRI 10 radiation quality reflect the difference in the inherent filtration of the x-ray tube used at each participant. For some radiation qualities the HVLs at the BARC are significantly different from the reference values. The very large deviations (up to 320 %) seen at the OAP when using the filtration recommended for the CCRI reference qualities might indicate a problem in the measurement of HVL. For the other participants, the HVLs of the CCRI reference radiation qualities, except for the CCRI 10 radiation quality, agree with the reference values within ± 5 %. The HVLs for the ISO 4037 narrow spectrum series are widely scattered but those of the INER, NMIJ/AIST and NIM, which have primary standards, agree within ± 5 %. The calibration coefficients for the participants whose HVLs deviate from the reference values by more than 10 % might need to be adjusted by applying radiation quality correction factors. However, no such correction was made in the present comparison because the NMIJ/AIST does not have enough data on the correction factors for each ionization chamber.

Table 12a. First half value layers for the CCRI radiation qualites and ISO 4037 narrow spectrum qualities given in mmAl but in mmCu for ISO N-40.

	CCRI 10	CCRI 30	CCRI 25	CCRI 50b	CCRI 50a	ISO N-15	ISO N-40
Reference value	0.037	0.169	0.242	1.017	2.262	0.14	0.084
NMIJ	0.039	0.169	0.243	1.017	2.264	0.14	0.082
NMIJ 52cm	0.032	0.169	0.242	1.017	2.263	N.A.	N.A.
Nuc. Malaysia	0.039	0.17	0.243	1.03	2.283	0.167	0.084
BARC	N.A.	0.204	0.263	1.033	2.273	0.16	0.071
ARPANSA 50cm	0.032	0.166	0.242	0.97	2.3	N.A.	N.A.
INER	0.039	0.17	0.242	1.006	2.279	0.134	0.086
OAP	0.072	0.53875	0.44787	1.7693	2.6176	0.208	0.088
AEC	N.A.	0.16	0.23	1	2.37	N.A.	N.A.
IAEA	0.037	0.163	0.232	0.997	2.371	N.A.	N.A.
NIM	0.043	0.172	0.252	1.018	2.284	0.135	0.084

Table 12b. First half value layers for the CCRI radiation qualites and ISO 4037 narrow spectrum qualities normalized to the reference value.

	CCRI 10	CCRI 30	CCRI 25	CCRI 50b	CCRI 50a	ISO N-15	ISO N-40
Reference value	1	1	1	1	1	1	1
NMIJ	1.05	1.00	1.00	1.00	1.00	1.00	0.98
NMIJ 52cm	0.86	1.00	1.00	1.00	1.00	N.A.	N.A.
Nuc. Malaysia	1.05	1.01	1.00	1.01	1.01	1.19	1.00
BARC	N.A.	1.21	1.09	1.02	1.00	1.14	0.85
ARPANSA 50cm	0.86	0.98	1.00	0.95	1.02	N.A.	N.A.
INER	1.05	1.01	1.00	0.99	1.01	0.96	1.02
OAP	1.95	3.19	1.85	1.74	1.16	1.49	1.05
AEC	N.A.	0.95	0.95	0.98	1.05	N.A.	N.A.
IAEA	1.00	0.96	0.96	0.98	1.05	N.A.	N.A.
NIM	1.16	1.02	1.04	1.00	1.01	0.96	1.00

4.4 Calibration coefficients

4.4.1 *Calibration coefficients for the CCRI reference radiation qualities*

The calibration coefficients and uncertainties for the CCRI reference radiation qualities obtained by the participants are listed in Tables 13 to 15 for the three transfer chambers and are also shown in Figures 6 to 8. The detailed uncertainty budgets for all the participants are given in Appendix C.

The calibration coefficients for the AE-1340C chamber at the BARC and the OAP were different from the other participants' results (by a factor of 15 at 10 kV). It was suspected that an extra cover to protect the front surface of the AE-1340C chamber was not removed in the measurements at these laboratories. To confirm the effect of the cover on the calibration coefficients, the AE-1340 chamber with the cover was calibrated at the NMIJ/AIST. As shown in figure 6b, the NMIJ (with cover) results come close to those at the BARC and OAP. In the following analysis, the BARC results for the AE-1340C chamber were compared to the NMIJ/AIST results measured with the protective cover in front of the chamber.

Regarding the OAP, as discussed above, the measured HVLs were quite different from those of the other institutes. In the following analysis, therefore, the calibration coefficients for the Magna and NE2536 chambers at the OAP were interpolated or extrapolated with respect to the HVLs at the NMIJ (the linking laboratory). The results for the Magna and NE2536 chambers are shown in Figure 5(a) and (b), respectively. An additional uncertainty of 2.0 % is included for the fitting procedure. From the fits, a set of values $N_{K,OAP}$(NMIJ HVL) was derived for the Magna and NE2536 chambers. It is these that have been used in the following analysis instead of the original values reported by the OAP. This fitting procedure was not applied to the results for the AE-1340C chamber at the OAP because of the problem with the protection cover as noted above.

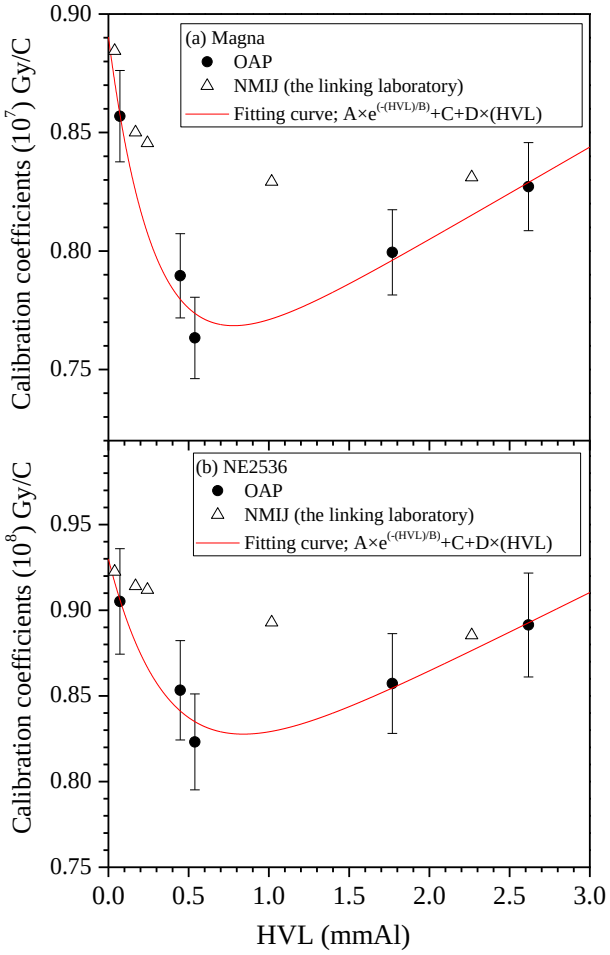

Figure 5. Calibration coefficients for (a) the Magna and (b) NE2536 chambers at the OAP (circle) and at the NMIJ (triangle). The red lines represent fitting curves to the OAP data.

Table 13. Calibration coefficients and relative standard uncertainties given by the participants for the transfer chamber Magna for the CCRI reference radiation qualities.

Participant, *i*	CCRI 10		CCRI 30		CCRI 25		CCRI 50b		CCRI 50a	
	$N_{k,i}$ (10^7 Gy/C)	u_i (%)	$N_{k,i}$ (10^7 Gy/C)	u_i (%)	$N_{k,i}$ (10^7 Gy/C)	u_i (%)	$N_{k,i}$ (10^7 Gy/C)	u_i (%)	$N_{k,i}$ (10^7 Gy/C)	u_i (%)
NMIJ	0.8845	0.40	0.8501	0.40	0.8456	0.40	0.8293	0.40	0.8311	0.40
Nuc. Malaysia	0.9238	0.58	0.8725	0.59	0.8662	0.58	0.8553	0.58	0.8542	0.58
BARC	N.A.		N.A.		N.A.		N.A.		N.A.	
INER	0.8837	0.59	0.8554	0.55	0.8477	0.54	0.8303	0.52	0.8338	0.53
OAP	0.8569	2.7	0.7634	2.7	0.7896	2.7	0.7995	2.7	0.8272	2.7
OAP(corrected HVL)	0.8715	3.4	0.8252	3.4	0.8076	3.4	0.7714	3.4	0.8152	3.4
AEC	N.A.		N.A.		N.A.		N.A.		N.A.	
IAEA	0.8893	0.40	0.8556	0.40	0.8488	0.40	0.8339	0.40	0.8354	0.40
NIM	0.8904	0.37	0.8556	0.37	0.8461	0.37	0.8314	0.37	0.8346	0.37
NMIJ (52cm)	0.9077	0.40	0.8598	0.40	0.8526	0.40	0.8384	0.40	0.8405	0.40
ARPANSA (50cm)	0.9023	0.70	0.8571	0.40	0.8515	0.40	0.8360	0.40	0.8400	0.40

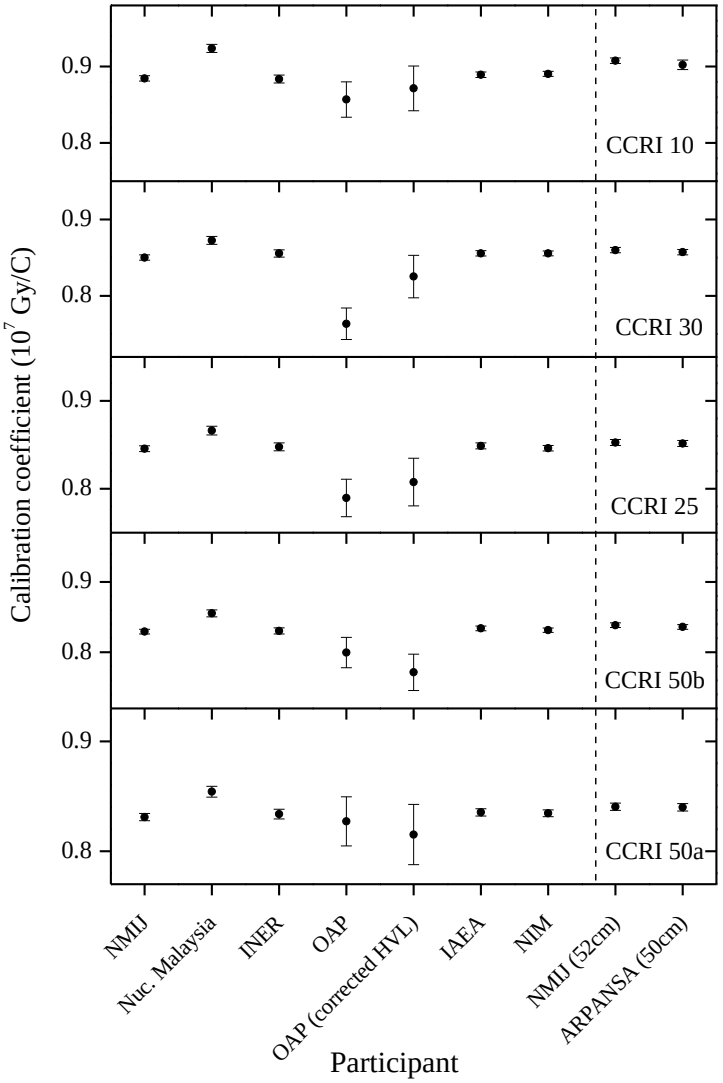

Figure 6. Calibration coefficients of the Magna transfer chamber for the CCRI radiation qualities.

Table 14. Calibration coefficients and relative standard uncertainties given by the participants for the transfer chamber AE-1340C for the CCRI reference radiation qualities.

Participant, *i*	CCRI 10		CCRI 30		CCRI 25		CCRI 50b		CCRI 50a	
	$N_{k,i}$ (10^8 Gy/C)	u_i (%)	$N_{k,i}$ (10^8 Gy/C)	u_i (%)	$N_{k,i}$ (10^8 Gy/C)	u_i (%)	$N_{k,i}$ (10^8 Gy/C)	u_i (%)	$N_{k,i}$ (10^8 Gy/C)	u_i (%)
NMIJ	1.1709	0.40	1.1034	0.40	1.0991	0.40	1.0971	0.40	1.1001	0.40
Nuc. Malaysia	1.2071	0.59	1.1259	0.58	1.1186	0.58	1.1277	0.58	1.1340	0.59
INER (positive)	1.1710	0.58	1.1144	0.55	1.1078	0.54	1.1032	0.52	1.1124	0.54
AEC	N.A.		1.0900	0.90	1.0730	0.90	1.0890	0.90	1.0880	0.90
IAEA	1.1719	0.40	1.1134	0.40	1.1054	0.40	1.1033	0.40	1.1052	0.40
NIM	1.1850	0.37	1.1190	0.37	1.1110	0.37	1.1100	0.37	1.1140	0.37
NMIJ (52cm)	1.2078	0.40	1.1127	0.40	1.1060	0.40	1.1049	0.40	1.1062	0.40
ARPANSA (50cm)	1.1819	0.70	1.1102	0.40	1.1033	0.40	1.1056	0.40	1.1117	0.40
NMIJ (with Cover)	14.765	0.64	2.2246	0.40	1.7567	0.40	1.2209	0.40	1.1322	0.40
BARC	N.A.		1.9841	0.82	1.7179	0.79	1.2148	0.81	1.1355	0.78
OAP	15.100	4.4	1.9000	4.4	1.6100	4.4	1.2000	4.4	1.1800	4.4

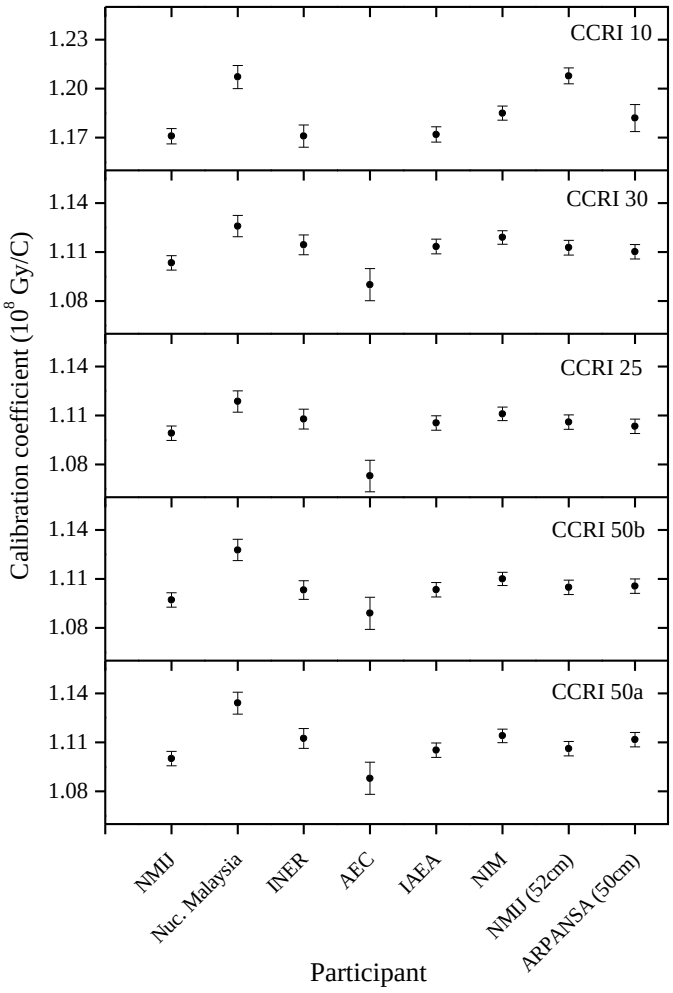

Figure 7a. Calibration coefficients of the AE-1340C transfer chamber for the CCRI radiation qualities (except for BARC and OAP).

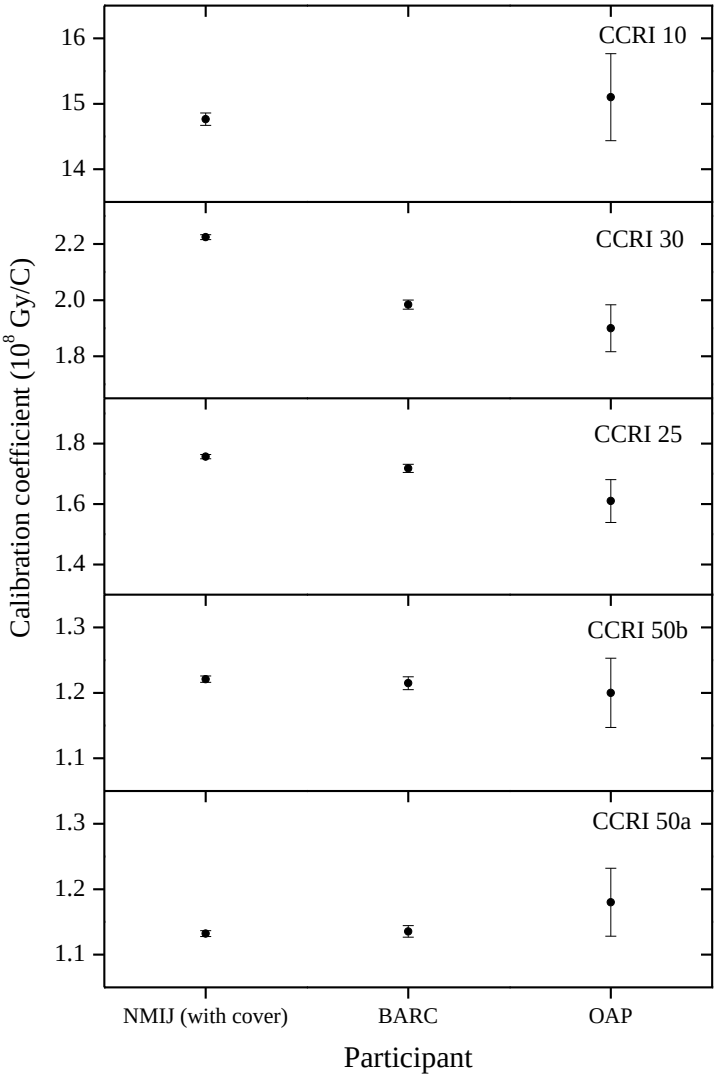

Figure 7b. Calibration coefficients of the AE-1340C transfer chamber with its protective cover for the CCRI radiation qualities (for NMIJ, BARC and OAP).

Table 15. Calibration coefficients and relative standard uncertainties given by the participants for the transfer chamber NE2536 for the CCRI reference radiation qualities.

Participant, *i*	CCRI 10		CCRI 30		CCRI 25		CCRI 50b		CCRI 50a	
	$N_{k,i}$ (10^8 Gy/C)	u_i (%)	$N_{k,i}$ (10^8 Gy/C)	u_i (%)	$N_{k,i}$ (10^8 Gy/C)	u_i (%)	$N_{k,i}$ (10^8 Gy/C)	u_i (%)	$N_{k,i}$ (10^8 Gy/C)	u_i (%)
NMIJ	0.9226	0.40	0.9141	0.40	0.9120	0.40	0.8929	0.40	0.8854	0.40
Nuc. Malaysia	0.9663	0.58	0.9389	0.58	0.9354	0.58	0.9209	0.58	0.9154	0.58
BARC	N.A.		1.0126	0.77	0.9924	0.77	0.9383	1.05	0.9048	0.81
INER	0.9303	0.56	0.9230	0.54	0.9177	0.53	0.8940	0.51	0.8878	0.52
OAP	0.9051	3.7	0.8232	3.7	0.8533	3.7	0.8572	3.7	0.8914	3.7
OAP (corrected HVL)	0.9163	4.2	0.8811	4.2	0.8666	4.2	0.8293	4.2	0.8765	4.2
NMIJ (after AEC)	0.9079	0.40	0.9007	0.40	0.8984	0.40	0.8786	0.40	0.8705	0.40
AEC	N.A.		0.8885	0.90	0.8974	0.90	0.8681	0.90	0.8592	0.90
IAEA	0.9123	0.40	0.8964	0.40	0.8949	0.40	0.8728	0.40	0.8638	0.40
NIM	0.9252	0.37	0.9099	0.37	0.9050	0.37	0.8759	0.37	0.8613	0.37
NMIJ (52cm)	0.9313	0.40	0.9214	0.40	0.9174	0.40	0.8991	0.40	0.8934	0.40
ARPANSA (50cm)	0.9407	0.70	0.9187	0.40	0.9145	0.40	0.8989	0.40	0.8903	0.40

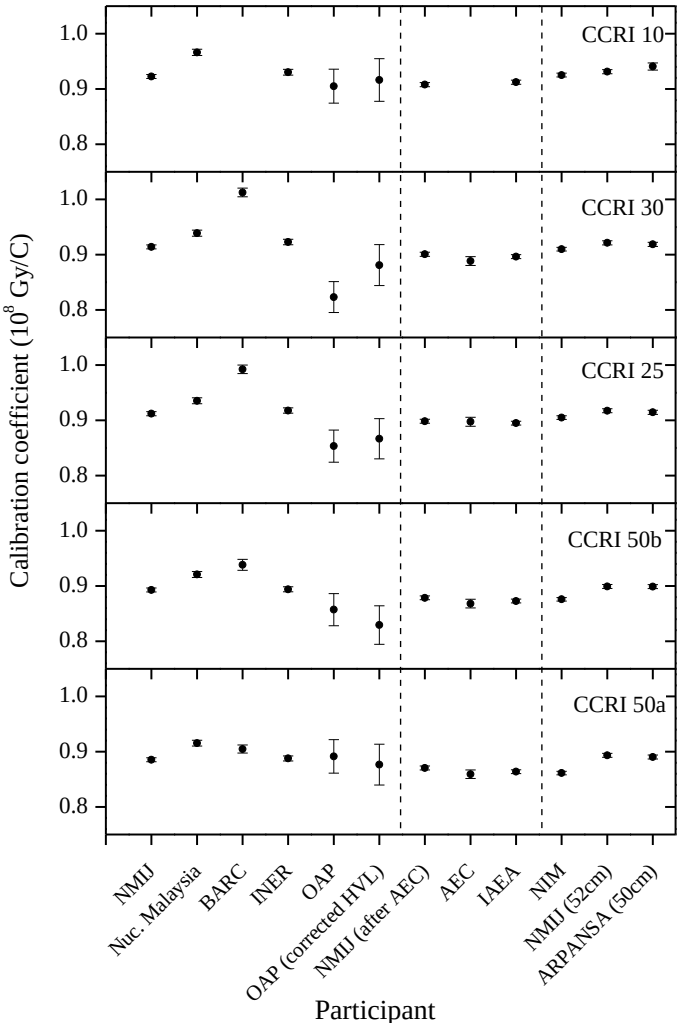

Figure 8. Calibration coefficients of the NE2536 transfer chamber for the CCRI radiation qualities.

Using the results of the NMIJ/AIST as the reference values for each radiation quality, the ratio of calibration coefficients of each chamber, $N_{k,i}/N_{k,\mathrm{NMIJ}}$, are evaluated as shown in Figure 9. Most calibration coefficients are in the range of ± 1 % (their uncertainties), however, some data deviate from the weighted mean values more than 10 %.

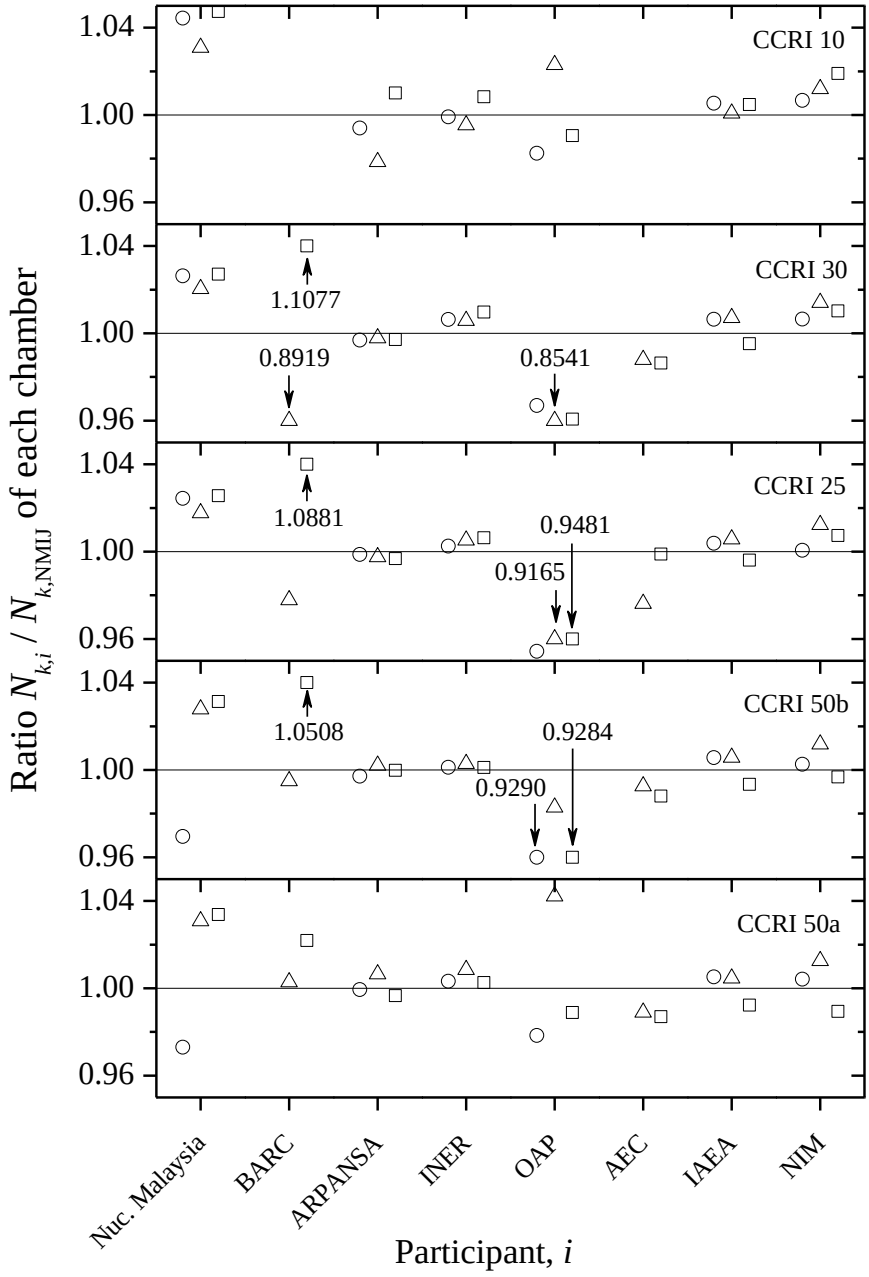

Figure 9. Ratio $N_{k,i}/N_{k,\mathrm{NMIJ}}$ of each transfer chamber for the CCRI radiation qualities; open circles: the Magna, open triangles: the AE-1340 (BARC and OAP using the protective cover), open squares: the NE2536.

The ratios $R_{\mathrm{NMI,BIPM}}$ for each CCRI radiation quality have been evaluated following the guidance

given in reference [7] using equation (1), the ratios $R_{\mathrm{NMI,Link}}$ evaluated from Tables 13 to 15 (where Link represents the NMIJ/AIST) and the ratios $R_{\mathrm{Link,BIPM}}$ given in Table 5. Weighted mean values using the weights u_{stab}, shown in Table 6, have been used to combine the data for the three transfer chambers. The final comparison result $R_{\mathrm{NMI,BIPM}}$ for each participant relative to the BIPM is given in Table 16 and Figure 10.

Table 16. Ratio $R_{\mathrm{NMI,\ BIPM}}$ between participants and the BIPM obtained using the values of the linking laboratory NMIJ/AIST shown in Table 5.

	CCRI 10		CCRI 30		CCRI 25		CCRI 50b		CCRI 50a	
Participant, *i*	$R_{i,BIPM}$	$u_{i,BIPM}$ (%)	$R_{i,BIPM}$	$u_{i,BIPM}$ (%)	$R_{i,BIPM}$	$u_{i,BIPM}$ (%)	$R_{i,BIPM}$	$u_{i,BIPM}$ (%)	$R_{i,BIPM}$	$u_{i,BIPM}$ (%)
Nuc. Malaysia	1.0420	0.70	1.0257	0.69	1.0259	0.69	1.0349	0.69	1.0370	0.70
BARC	N.A.		1.01	5.0	1.04	5.0	1.03	5.0	1.019	5.0
ARPANSA	0.9966	0.85	0.9983	0.61	1.0007	0.61	1.0046	0.61	1.0060	0.61
INER	1.0028	0.67	1.0086	0.67	1.0083	0.67	1.0064	0.67	1.0102	0.67
OAP	0.991	3.9	0.967	3.6	0.955	3.6	0.934	4.0	0.992	4.0
AEC	N.A.		0.9880	0.98	0.9921	0.98	0.9946	0.98	0.9933	0.98
IAEA	1.0045	0.54	1.0028	0.54	1.0043	0.54	1.0049	0.54	1.0048	0.54
NIM	1.0147	0.62	1.0117	0.62	1.0107	0.62	1.0078	0.62	1.0061	0.62

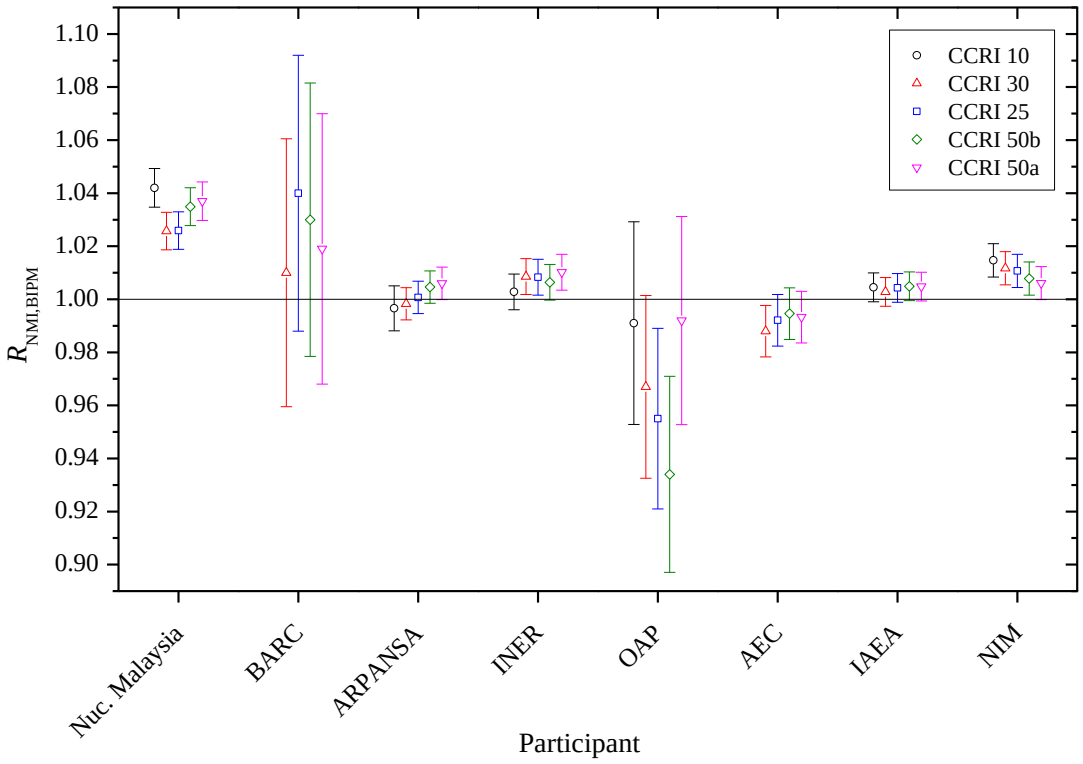

Figure 10. Ratio $R_{\mathrm{NMI,BIPM}}$ for each participating laboratory for APMP. RI(I)-K2 comparison. The uncertainty bars represent the standard uncertainty (k = 1).

The combined standard uncertainty $u_{\mathrm{NMI,BIPM}}$ of $R_{\mathrm{NMI,BIPM}}$ for each laboratory is also given in Table 16. The uncertainty has six components: (i) the laboratory calibration uncertainty as given in Appendix C; (ii) the BIPM uncertainty (0.2 %) (described in table 2 of reference [8]); (iii) the

uncertainty u_{stab} arising from the stability of the transfer chambers, where u_{stab} = 0.11 % for the Magna, 0.09 % for the AE-1340 and 0.08 % for the NE2536, giving the combined value u_{stab} = 0.05 %; (iv) the uncertainty associated with ion recombination (0.1 %); (v) the procedural uncertainty u_{Link} associated with chamber positioning, ionization current measurements and normalization to standard air density at the NMIJ; and (vi) the spread of the results for the different transfer chambers. This latter component is particularly important for the BARC, who measured only two of the three transfer chambers and obtained the mean result $R_{BARC,BIPM}$ = 1.01 at 30 kV despite the fact that the results for the two chambers differed by over 20 %.

Correlation in the laboratory and BIPM standards is removed from this total. As the AEC and the IAEA are both traceable to the BIPM, the combined uncertainty of the non-statistical components for the BIPM (0.2 %) do not enter in the calculation of u_i for these laboratories. The physical constants ρ_{air} and W_{air}/e, and certain correction factors (k_h and $1-g_{air}$) for the free air chambers of the ARPANSA, BARC, INER, NIM and the BIPM are fully correlated, while for the correlation factors k_e and k_{sc} only half the uncertainty is included.

4.4.2 *Calibration coefficients for the ISO 4037 narrow spectrum series*

The calibration coefficients and uncertainties for the ISO 4037 narrow spectrum series obtained by the participants are listed in Tables 17 to 19 and are also shown in Figures 11 to 13 (see also Appendix C for the detailed uncertainty budgets for all the participants).

Table 17. Calibration coefficients and relative standard uncertainties for the ISO 4037 narrow spectrum series given by the participants for the transfer chamber Magna.

Participant, i	ISO N-15		ISO N-40	
	$N_{k,i}$ (10^7 Gy/C)	u_i (%)	$N_{k,i}$ (10^7 Gy/C)	u_i (%)
NMIJ	0.8575	0.41	0.8328	0.41
Nuc. Malaysia	0.8629	0.58	0.8146	0.58
BARC	N.A.		N.A.	
ARPANSA	N.A.		N.A.	
INER	0.8608	0.64	0.8354	0.62
OAP	0.8507	2.3	0.7026	2.3
AEC	N.A.		N.A.	
IAEA	N.A.		N.A.	
NIM	0.8673	0.37	0.8358	0.37

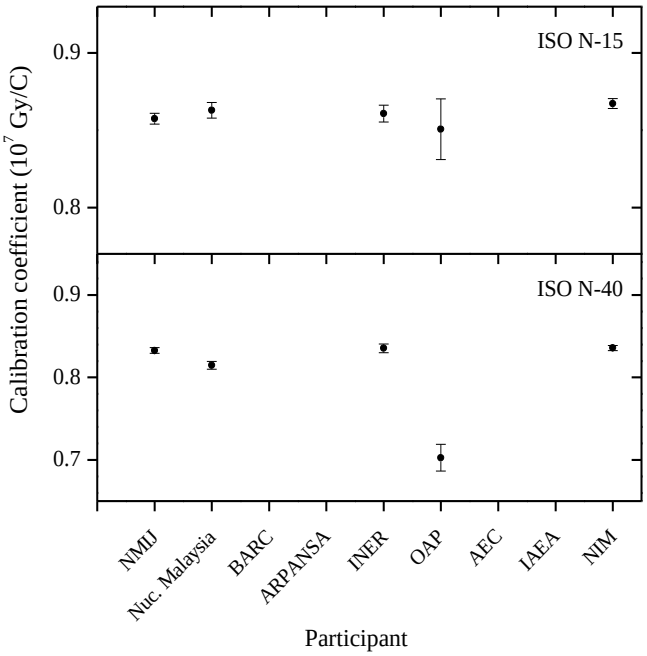

Figure 11. Calibration coefficients of the Magna transfer chamber for the ISO 4037 narrow spectrum series (ISO N-15 and N-40).

Table 18. Calibration coefficients and relative standard uncertainties for the ISO 4037 narrow spectrum series given by the participants for the transfer chamber AE-1340C.

Participant, i	ISO N-15		ISO N-40	
	$N_{k,i}$ (10^8 Gy/C)	u_i (%)	$N_{k,i}$ (10^8 Gy/C)	u_i (%)
NMIJ	1.1087	0.56	1.1083	0.64
Nuc. Malaysia	1.0631	0.71	1.0930	0.82
ARPANSA	N.A.		N.A.	
INER	1.1150	0.63	1.1121	0.58
AEC	N.A.		N.A.	
IAEA	N.A.		N.A.	
NIM	1.1260	0.37	1.1130	0.47
NMIJ (with cover)	2.3280	0.56	1.1095	0.64
BARC	2.2960	1.46	1.1414	0.99
OAP	1.9800	4.2	0.9880	4.2

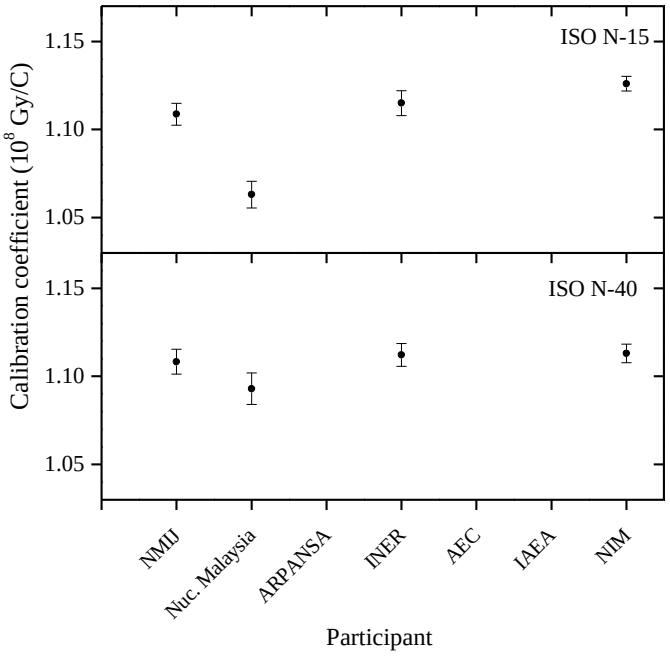

Figure 12(a). Calibration coefficients of the AE-1340C transfer chamber for the ISO 4037 narrow spectrum series (ISO N-15 and N-40).

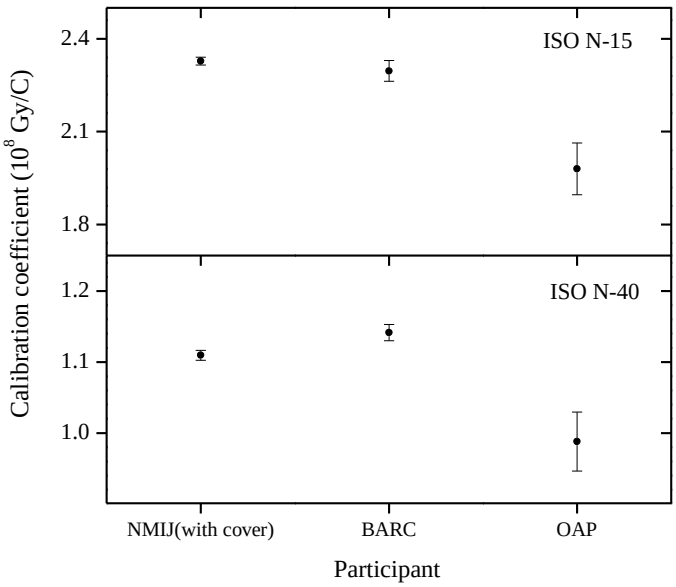

Figure 12(b). Calibration coefficients of the AE-1340C transfer chamber with the protective cover for the ISO 4037 narrow spectrum series (ISO N-15 and N-40).

Table 19. Calibration coefficients and relative standard uncertainties for the ISO 4037 narrow spectrum series given by the participants for the transfer chamber NE 2536.

Participant, i	ISO N-15		ISO N-40	
	$N_{k,i}$ (10^8 Gy/C)	u_i (%)	$N_{k,i}$ (10^8 Gy/C)	u_i (%)
NMIJ	0.9229	0.56	0.8874	0.56
Nuc. Malaysia	0.9724	0.58	1.1534	0.58
BARC	1.0065	1.10	0.8863	1.01
ARPANSA	N.A.		N.A.	
INER	0.9301	0.62	0.8948	0.56
OAP	0.8975	3.4	0.7535	3.4
NMIJ (after AEC)	0.9078	0.6	0.8738	0.6
AEC	N.A.		N.A.	
IAEA	N.A.		N.A.	
NIM	0.9231	0.37	0.8649	0.47

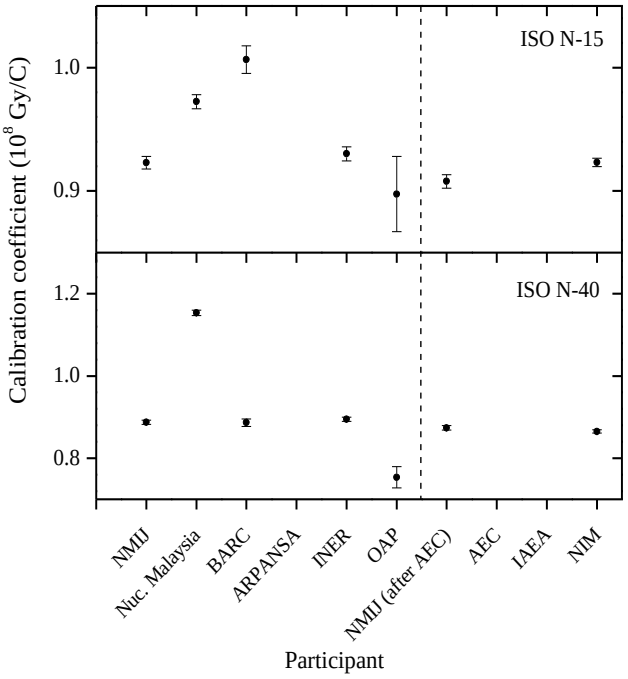

Figure 13. Calibration coefficients of the NE2536 transfer chamber for the ISO 4037 narrow spectrum series (ISO N-15 and N-40).

Significant deviations are observed in Figures 11, 12 and 13, as for the CCRI radiation qualities. Consequently, weighted mean values of the results at the INER, NMIJ/AIST and NIM are used as the reference values. Using these weighted mean values for each transfer chamber as the reference values for each radiation quality, the relative deviations from the weighted mean values are evaluated as shown in Figure 14. Most calibration coefficients are in the range of ± 1 %, however,

some values deviate from the weighted mean by more than 10 %, as observed for the CCRI radiation qualities, and one result (Nuclear Malaysia, ISO-N40, NE2536) deviates by more than 30 %.

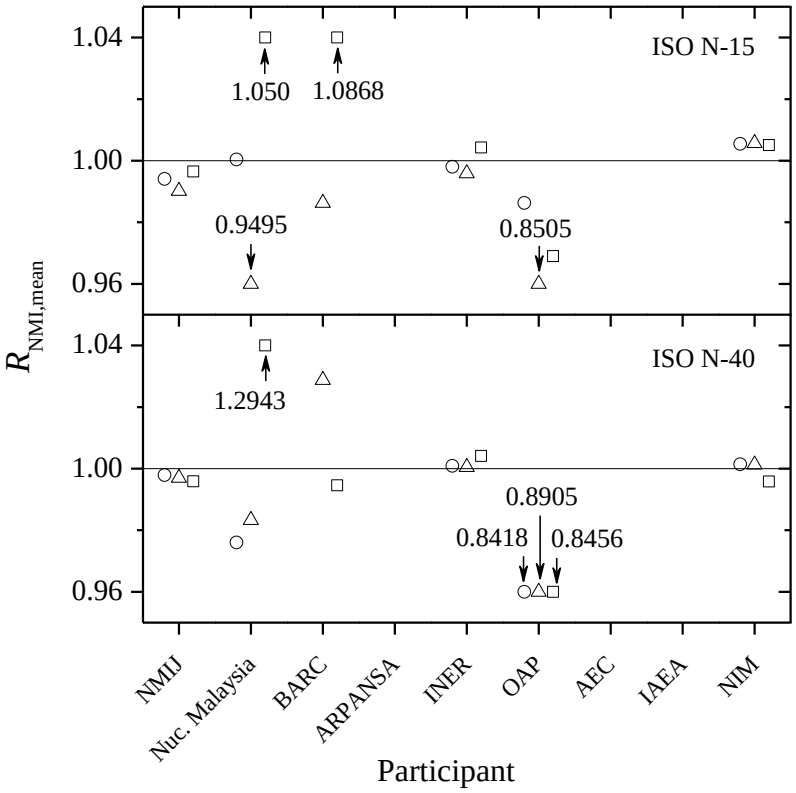

Figure 14. Ratio $R_{NMI,mean}$ of each transfer chamber for the ISO 4037 narrow spectrum series; open circles: the Magna, open triangles: the AE-1340, open squares: the NE2536.

Note that no link can be made to the BIPM as there is no key comparison for ISO narrow qualities. However, regional reference values were evaluated for these qualities as the weighted mean of the $R_{NMI,mean}$ for the three transfer chambers. The final comparison result $R_{NMI,regional}$ for each participant relative to the regional reference values is given in Table 20 and Figure 15.

The combined standard uncertainty $u_{NMI,regional}$ of $R_{NMI,regional}$ for each laboratory is also given in Table 20. The uncertainty has five components: (i) the laboratory calibration uncertainty as given in Appendix C; (ii) the calibration uncertainty u_{Link} at the linking laboratory (NMIJ/AIST); (iii) the uncertainty u_{stab} arising from the stability of the transfer chambers u_{stab} = 0.05 %; (iv) the uncertainty associated with the ion recombination (0.2 %); and (v) the spread of the results for the different transfer chambers.

Correlation in the laboratory and the linking laboratory (the NMIJ/AIST) standards is removed from this total; this includes the physical constants ρ_{air} and W_{air}/e, and certain correction factors (full correlation; k_h and 1-$g_{air,}$ half correlation; k_e and k_{sc}) for the free air chambers of the BARC, INER, NIM and the NMIJ/AIST.

Table 20. Ratio $R_{\mathrm{NMI,\ regional}}$ between participants and the regional reference values for the ISO 4037 narrow spectrum series (ISO N-15 and N-40).

	N-15 kV		N-40 kV	
Participant, *i*	$R_{NMI,regional}$	$u_{i,regional}$ (%)	$R_{NMI,regional}$	$u_{i,regional}$ (%)
NMIJ	0.9936	0.64	0.9969	0.66
Nuc. Malaysia	1.00	6.3	1.08	6.3
BARC	1.04	3.4	1.01	3.4
ARPANSA	N.A.	N.A.	N.A.	N.A.
INER	0.9994	0.68	1.0018	0.68
OAP	0.94	3.7	0.86	3.7
AEC	N.A.	N.A.	N.A.	N.A.
IAEA	N.A.	N.A.	N.A.	N.A.
NIM	1.0054	0.59	0.9995	0.62

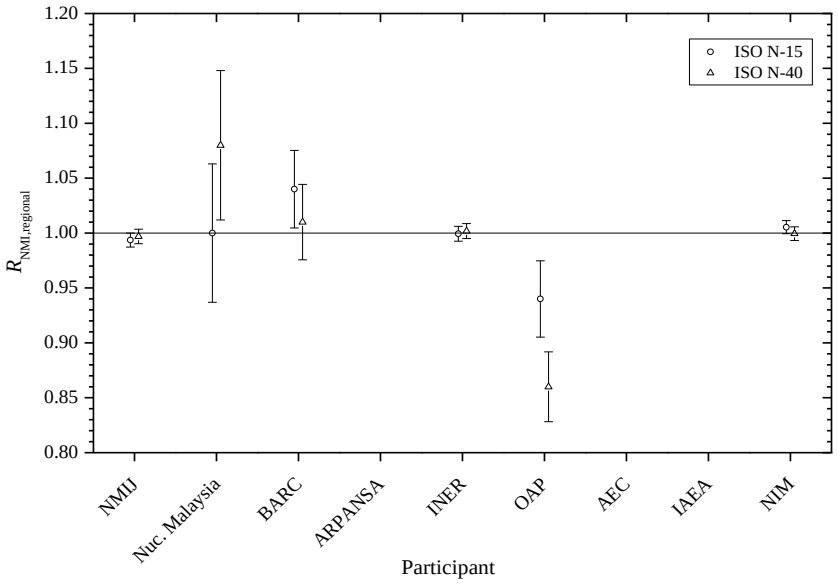

Figure 15. Ratio $R_{\mathrm{NMI,regional}}$ for each participating laboratory for the ISO narrow spectrum series (ISO N-15 and N-40). The uncertainty bars represent the standard uncertainty (k = 1).

5. Degrees of equivalence

The analysis of the results of BIPM comparisons for low-energy x-rays in terms of degrees of equivalence is described in reference [8]. Following a decision of the CCRI, the BIPM determination of air kerma is taken as the key comparison reference value $x_{R,i}$, for each of the CCRI radiation qualities. It follows that for each NMI i having comparison result $R_{i,\mathrm{BIPM}}$ (denoted in

earlier sections as $R_{\mathrm{NMI,BIPM}}$) with combined standard uncertainty $u_{i,\mathrm{BIPM}}$, (as given in Table 16), the degree of equivalence with respect to the reference value is the difference $D_i = R_{i,\mathrm{BIPM}} - 1$ and its expanded uncertainty $U_i = 2\ u_{i,\mathrm{BIPM}}$. The results for D_i and U_i are shown in Table 21 and Figure 16. Unfortunately, the results for the AEC cannot be included in the BIPM key comparison database as the AEC is not a designated institute for dosimetry.

Table 21. Degree of equivalence D_i and its expanded uncertainty U_i of each participant.

Participant, *i*	10 kV		30 kV		25 kV		50 kVb		50 kVa	
	D_i (mGy/Gy)	U_i	D_i (mGy/Gy)	U_i	D_i (mGy/Gy)	U_i	D_i (mGy/Gy)	U_i	D_i (mGy/Gy)	U_i
NMIJ*	0.9	3.6	1.0	3.6	3.2	3.6	4.6	3.6	5.4	3.6
Nuc. Malaysia	42.0	14.0	25.7	13.9	25.9	13.9	34.9	13.9	37.0	14.0
BARC	N. A.	N. A.	13.5	100	42.8	100	30.9	101	19.0	100
INER	2.8	13.4	8.6	13.4	8.3	13.4	6.4	13.4	10.2	13.4
OAP	-8.7	77	-32.7	71	-45.0	71	-66.5	79	-7.9	79
AEC	N. A.	N. A.	-12.0	19.6	-7.9	19.6	-5.4	19.6	-6.7	19.6
IAEA	4.5	10.8	2.8	10.8	4.3	10.8	4.9	10.8	4.8	10.8
NIM	14.7	12.4	11.7	12.4	10.7	12.4	7.8	12.4	6.1	12.4

* from the KCDB

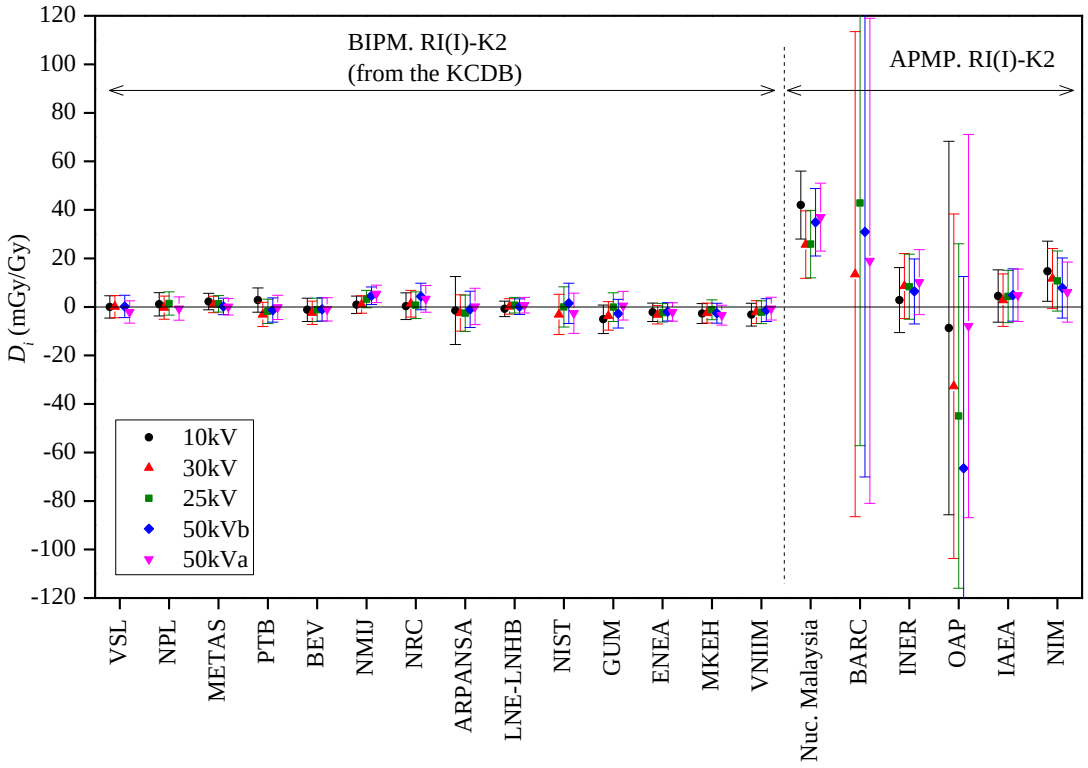

Figure 16. Degree of equivalence D_i and U_i for each NMI *i* with respect to the key comparison reference value.

The results for the ARPANSA have not been used to evaluate new degrees of equivalence. The ARPANSA undertook a BIPM key comparison in November 2008 [9] resulting in the degrees of equivalence presently available in the BIPM key comparison database. These degrees of equivalence

will not be updated because the uncertainties in the new comparison are larger (mainly because the regional comparison is less direct). Usually in these circumstances the ARPANSA would be a linking laboratory, and the issue of updating degrees of equivalence with less precise values would not arise. As already noted, however, the status of ARPANSA was changed from a linking laboratory to that of a participant because of the different source-detector distance used.

6. Conclusions

This comparison of air kerma measurement standards piloted by the NMIJ/AIST is the first to be conducted in the Asia-Pacific region using the CCRI reference radiation qualities from 10 kV to 50 kV and the ISO 4037 narrow spectrum series (15 kV and 40 kV). Complications caused by deviations from the protocol at several laboratories were remedied by additional measurements at the NMIJ/AIST. A step change in one of the chambers during the course of the comparison also complicated the analysis, and there was poor matching of the reference HVLs at the OAP and at the BARC (below 50 kV).

For the CCRI reference qualities (Table 16 and Figure 10) there is general agreement within the combined uncertainties, although the results for Nuclear Malaysia and for the OAP at 30 kV, 25 kV and 50kVb show larger differences. The results for the BARC at 30 kV are also notable in that they obtained values differing by more than 20 % for the two transfer chambers measured, although fortuitously the mean value falls close to unity. As noted earlier, the combined standard uncertainty $u_{i,\mathrm{BIPM}}$ includes a component for differences between transfer chambers and it is noted that the use of the present report to support calibration and measurement capabilities should be viewed in the context of the expanded uncertainty that will appear in the key comparison database. For the ISO qualities (Table 20 and Figure 15), most results are in reasonable agreement with the regional mean values, except perhaps for the OAP at the N-40 quality.

References

[1] BIPM, Qualités de rayonnement, 1972, CCEMRI(I), R15.

[2] ISO 4037-1, X and gamma reference radiation for calibrating dosemeters and doserate meters and for determining their response as a function of photon energy – Part 1: Radiation characteristics and production methods, 1996.

[3] “Guide to the Expression of Uncertainty in Measurement”, International Organization of Standards, Switzerland (1995).

[4] CIPM, *Measurement comparisons in the CIPM MRA*, CIPM MRA-D-05, 2013, BIPM, 29 pp.

[5] D T Burns, A Nohtomi, N Saito, T Kurosawa, N Takata, “Key comparison BIPM.RI(I)-K2 of air-kerma standards of the NMIJ and the BIPM in low-energy x-rays”, *Metrologia* **45** (2008) *Tech. Suppl*. 06015.

[6] D T Burns, C Kessler and J P McCaffrey, "Key comparison BIPM.RI(I)-K2 of air-kerma standards of the NRC, Canada and the BIPM in low-energy x-rays", *Metrologia* **48** (2011) *Tech. Suppl.* 06002.

[7] D T Burns and P J Allisy-Robers, The evaluation of degrees of equivalence in regional dosimetry comparisons, 2007, *CCRI(I)/07-04*.

[8] D T Burns, "Degrees of equivalence for the key comparison BIPM.RI(I)-K2 between national primary standards for low-energy x-rays", Summary report for BIPM.RI(I)-K2 2003-09-24.

[9] D T Burns, J E Lye, C Kessler, P Roger and D J Butler, "Key comparison BIPM.RI(I)-K2 of the air-kerma standards of the ARPANSA and the BIPM in low-energy x-rays", *Metrologia* **47** (2010) *Tech. Suppl.* 06023.

APPENDIX A: Photographs of the transfer chambers

1. EXRADIN Magna, Serial number D070313

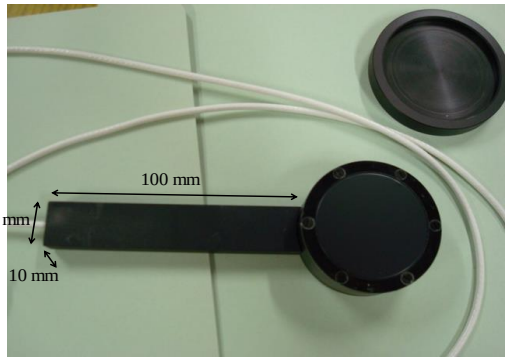

2. OYOGIKEN AE-1340C, Serial number 1042

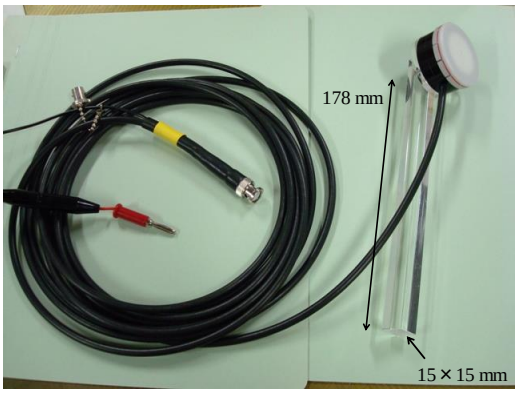

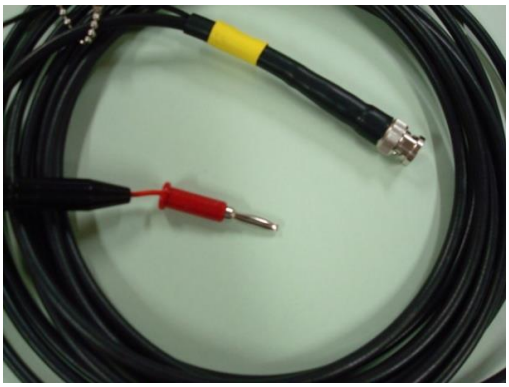

3. NE 2536/3, Serial number R17804

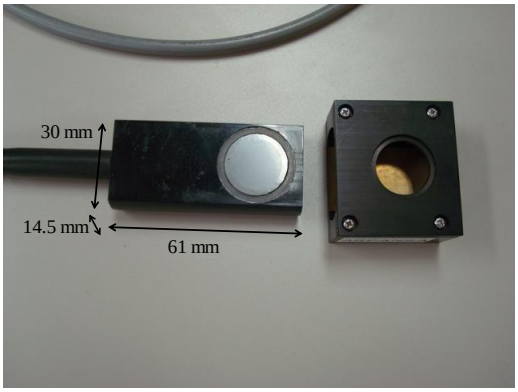

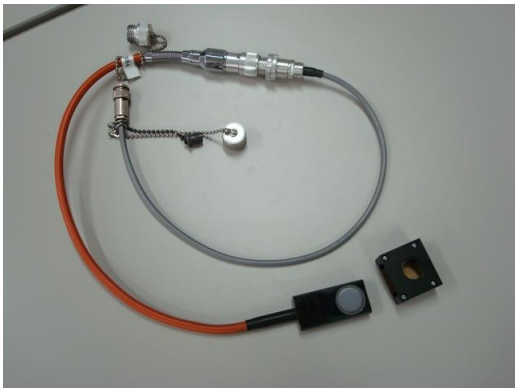

APPENDIX B: Damage in the NE2536 chamber

Jul. 2008

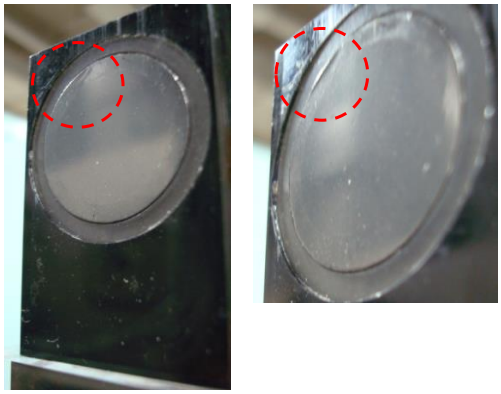

Jul. 2010

APPENDIX C: Tables of the uncertainty budgets for each participant

Table C1. AEC uncertainty budget

Uncertainty associated with the standard

Source of component	**Relative standard uncertainty (%)**	
	Type A	**Type B**
Air kerma rate		
N_k from PSDL		0.50
Distance		0.06
Current measurement	0.67	
Electrometer resolution		0.02
Temperature	0.01	
Pressure	0.01	0.01
Humidity		0.10
Quadratic sum	0.67	0.51
Combined standard uncertainty	0.84	

Uncertainty associated with the calibration of the transfer chambers

Transfer chambers →	**AE-1340C**		**NE 2536**	
Source of component	**Relative standard uncertainty (%)**		**Relative standard uncertainty (%)**	
	Type A	**Type B**	**Type A**	**Type B**
Air kerma rate	0.67	0.51	0.67	0.51
Charge measurement	0.21		0.19	
Temperature	0.00	0.00	0.00	0.00
Pressure	0.01	0.01	0.01	0.01
Distance		0.06		0.06
Quadratic sum	0.70	0.52	0.70	0.52
Combined standard uncertainty	0.87		0.87	

Table C2a. ARPANSA uncertainty budget (CCRI 10)

Uncertainty associated with the standard

Source of component	Relative standard uncertainty (%)	
	Type A	Type B
Physical constants		
$1\text{-}g_{air}$		0.01
Correction factors		
Scattered radiation		0.02
Fluoresence		0.04
Electron loss		0.03
Ion recombination		0.01
Polarity		0.05
Air attenuation		0.60
Field distortion		0.05
Transmission through edges of diaphragm		0.01
Scattering from diahragm		0.00
Wall transmission		0.00
Humidity		0.03
Other correction factor		
Beam non-uniformity		0.10
Volume and current measurement		
Volume		0.03
Current measurement	0.05	
Distance		0.20
Temperature		0.20
Pressure		0.01
Quadratic sum	0.05	0.68
Combined standard uncertainty	0.68	

Uncertainty associated with the calibration of the transfer chambers

Transfer chambers →	AE-1340C		NE 2536		Magna	
Source of component	Relative standard uncertainty (%)		Relative standard uncertainty (%)		Relative standard uncertainty (%)	
	Type A	Type B	Type A	Type B	Type A	Type B
Air kerma rate	0.05	0.68	0.05	0.68	0.05	0.68
Current measurement	0.08		0.10		0.05	
Temperature		0.20		0.20		0.20
Pressure		0.01		0.01		0.01
Humidity		0.03		0.03		0.03
Quadratic sum	0.09	0.71	0.11	0.71	0.07	0.71
Combined standard uncertainty	0.71		0.72		0.71	

Table C2b. ARPANSA uncertainty budget (CCRI 30, 25, 50b and 50a)

Uncertainty associated with the standard

Source of component	Relative standard uncertainty (%)	
	Type A	Type B
Physical constants		
$1\text{-}g_{air}$		0.01
Correction factors		
Scattered radiation		0.02
Fluoresence		0.04
Electron loss		0.03
Ion recombination		0.01
Polarity		0.05
Air attenuation		0.10
Field distortion		0.05
Transmission through edges of diaphragm		0.01
Scattering from diahragm		0.00
Wall transmission		0.00
Humidity		0.03
Other correction factor		
Beam non-uniformity		0.10
Volume and current measurement		
Volume		0.03
Current measurement	0.05	
Distance		0.20
Temperature		0.20
Pressure		0.01
Quadratic sum	0.05	0.33
Combined standard uncertainty	0.34	

Uncertainty associated with the calibration of the transfer chambers

Transfer chambers →	AE-1340C		NE 2536		Magna	
Source of component	**Relative standard uncertainty (%)**		**Relative standard uncertainty (%)**		**Relative standard uncertainty (%)**	
	Type A	**Type B**	**Type A**	**Type B**	**Type A**	**Type B**
Air kerma rate	0.05	0.33	0.05	0.33	0.05	0.33
Current measurement	0.08		0.10		0.05	
Temperature		0.20		0.20		0.20
Pressure		0.01		0.01		0.01
Humidity		0.03		0.03		0.03
Quadratic sum	0.09	0.39	0.11	0.39	0.07	0.39
Combined standard uncertainty	0.40		0.40		0.40	

Table C3a. BARC uncertainty budget (CCRI 30)

Uncertainty associated with the standard

Source of component	Relative standard uncertainty (%)	
	Type A	Type B
Physical constants		
Dry air density		0.01
W_{air}/e		0.15
Correction factors		
Ion recombination		0.10
Air attenuation		0.13
Volume and current measurement		
Volume		0.64
Current measurement	0.05	0.20
Distance		0.23
Temperature		0.02
Pressure		0.01
Quadratic sum	0.05	0.74
Combined standard uncertainty	0.74	

Uncertainty associated with the calibration of the transfer chambers

Transfer chambers →	AE-1340C		NE 2536	
Source of component	Relative standard uncertainty (%)		Relative standard uncertainty (%)	
	Type A	Type B	Type A	Type B
Air kerma rate	0.05	0.74	0.05	0.74
Current measurement	0.04	0.22	0.02	0.21
Temperature	0.26	0.02		0.02
Pressure		0.01		0.01
Quadratic sum	0.27	0.78	0.05	0.77
Combined standard uncertainty	0.82		0.77	

Table C3b. BARC uncertainty budget (CCRI 25)

Uncertainty associated with the standard

Source of component	Relative standard uncertainty (%)	
	Type A	Type B
Physical constants		
Dry air density		0.01
W_{air}/e		0.15
Correction factors		
Ion recombination		0.10
Air attenuation		0.11
Volume and current measurement		
Volume		0.64
Current measurement	0.03	0.21
Distance		0.23
Temperature		0.02
Pressure		0.01
Quadratic sum	0.03	0.74
Combined standard uncertainty	0.74	

Uncertainty associated with the calibration of the transfer chambers

Transfer chambers →	**AE-1340C**		**NE 2536**	
Source of component	**Relative standard uncertainty (%)**		**Relative standard uncertainty (%)**	
	Type A	**Type B**	**Type A**	**Type B**
Air kerma rate	0.03	0.74	0.03	0.74
Current measurement	0.07	0.20	0.04	0.20
Temperature	0.17	0.02	0.08	0.02
Pressure		0.01	0.01	0.01
Quadratic sum	0.19	0.77	0.09	0.77
Combined standard uncertainty	0.79		0.78	

Table C3c. BARC uncertainty budget (CCRI 50b)

Uncertainty associated with the standard

Source of component	Relative standard uncertainty (%)	
	Type A	Type B
Physical constants		
Dry air density		0.01
W_{air}/e		0.15
Correction factors		
Ion recombination		0.10
Air attenuation		0.03
Volume and current measurement		
Volume		0.64
Current measurement	0.03	0.20
Distance		0.23
Temperature		0.02
Pressure	0.01	0.01
Quadratic sum	0.03	0.73
Combined standard uncertainty	0.73	

Uncertainty associated with the calibration of the transfer chambers

Transfer chambers →	AE-1340C		NE 2536	
Source of component	Relative standard uncertainty (%)		Relative standard uncertainty (%)	
	Type A	Type B	Type A	Type B
Air kerma rate	0.03	0.73	0.03	0.73
Current measurement	0.04	0.23	0.09	0.22
Temperature	0.25	0.02	0.72	0.02
Pressure	0.01	0.01		0.01
Quadratic sum	0.26	0.77	0.73	0.77
Combined standard uncertainty	0.81		1.05	

Table C3d. BARC uncertainty budget (CCRI 50a)

Uncertainty associated with the standard

Source of component	Relative standard uncertainty (%)	
	Type A	Type B
Physical constants		
Dry air density		0.01
W_{air}/e		0.15
Correction factors		
Ion recombination		0.10
Air attenuation		0.02
Volume and current measurement		
Volume		0.64
Current measurement	0.04	0.20
Distance		0.23
Temperature	0.14	0.02
Pressure	0.01	0.01
Quadratic sum	0.15	0.73
Combined standard uncertainty	0.75	

Uncertainty associated with the calibration of the transfer chambers

Transfer chambers →	**AE-1340C**		**NE 2536**	
Source of component	**Relative standard uncertainty (%)**		**Relative standard uncertainty (%)**	
	Type A	**Type B**	**Type A**	**Type B**
Air kerma rate	0.15	0.73	0.15	0.73
Current measurement	0.06	0.21	0.04	0.20
Temperature	0.00	0.02	0.25	0.02
Pressure	0.01	0.01		0.01
Quadratic sum	0.16	0.76	0.29	0.76
Combined standard uncertainty	0.78		0.81	

Table C3e. BARC uncertainty budget (ISO N-15)

Uncertainty associated with the standard

Source of component	Relative standard uncertainty (%)	
	Type A	Type B
Physical constants		
Dry air density		0.01
W_{air}/e		0.15
Correction factors		
Ion recombination		0.10
Air attenuation		0.15
Volume and current measurement		
Volume		0.64
Current measurement	0.03	0.20
Distance		0.23
Temperature		0.02
Pressure	0.01	0.01
Quadratic sum	0.03	0.75
Combined standard uncertainty	0.75	

Uncertainty associated with the calibration of the transfer chambers

Transfer chambers →	AE-1340C		NE 2536	
Source of component	Relative standard uncertainty (%)		Relative standard uncertainty (%)	
	Type A	Type B	Type A	Type B
Air kerma rate	0.03	0.75	0.03	0.75
Current measurement	0.90	0.81	0.41	0.40
Temperature	0.34	0.02	0.57	0.02
Pressure	0.01	0.01		0.01
Quadratic sum	0.96	1.10	0.70	0.85
Combined standard uncertainty	1.46		1.10	

Table C3f. BARC uncertainty budget (ISO N-40)

Uncertainty associated with the standard

Source of component	**Relative standard uncertainty (%)**	
	Type A	**Type B**
Physical constants		
Dry air density		0.01
W_{air}/e		0.15
Correction factors		
Ion recombination		0.10
Air attenuation		0.02
Volume and current measurement		
Volume		0.64
Current measurement	0.16	0.20
Distance		0.23
Temperature	0.29	0.02
Pressure	0.01	0.01
Quadratic sum	0.33	0.73
Combined standard uncertainty	0.80	

Uncertainty associated with the calibration of the transfer chambers

Transfer chambers →	**AE-1340C**		**NE 2536**	
Source of component	**Relative standard uncertainty (%)**		**Relative standard uncertainty (%)**	
	Type A	**Type B**	**Type A**	**Type B**
Air kerma rate	0.33	0.73	0.33	0.73
Current measurement	0.27	0.45	0.28	0.38
Temperature	0.25	0.02	0.40	0.02
Pressure		0.01		0.01
Quadratic sum	0.50	0.86	0.59	0.83
Combined standard uncertainty	0.99		1.01	

Table C4. IAEA uncertainty budget

Uncertainty associated with the standard

Source of component	Relative standard uncertainty (%)	
	Type A	Type B
Air kerma rate		
N_k from BIPM (or PSDL)		0.21
Long term stability of the secondary standard		0.20
Current measurement	0.05	0.04
Monitor		0.10
Temperature	0.01	0.03
Pressure	0.05	0.06
Quadratic sum	0.07	0.32
Combined standard uncertainty	0.32	

Uncertainty associated with the calibration of the transfer chambers

Transfer chambers →	AE-1340C		NE 2536		Magna	
Source of component	Relative standard uncertainty (%)		Relative standard uncertainty (%)		Relative standard uncertainty (%)	
	Type A	Type B	Type A	Type B	Type A	Type B
Air kerma rate	0.07	0.32	0.07	0.32	0.07	0.32
Current measurement	0.05	0.04	0.05	0.04	0.05	0.04
Temperature	0.01	0.03	0.01	0.03	0.01	0.03
Pressure	0.05	0.06	0.05	0.06	0.05	0.06
Distance		0.01		0.01		0.01
Monitor		0.10		0.10		0.10
Quadratic sum	0.10	0.34	0.10	0.34	0.10	0.34
Combined standard uncertainty	0.36		0.36		0.36	

Table C5. INER uncertainty budget

Uncertainty associated with the standard

Source of component	Relative standard uncertainty (%)	
	Type A	Type B
Physical constants		
Dry air density		0.01
W_{air}/e		0.15
Correction factors		
Scattered radiation		0.10
Electron loss		0.05
Ion recombination	0.15	
Air attenuation		0.10
Humidity		0.10
Volume and current measurement		
Volume		0.12
Current measurement	0.05	0.05
Distance	0.01	0.03
Temperature	0.01	0.20
Pressure	0.01	0.10
Quadratic sum	0.16	0.35
Combined standard uncertainty	0.38	

Uncertainty associated with the calibration of the transfer chambers

Transfer chambers →	AE-1340C		NE 2536		Magna	
Source of component	Relative standard uncertainty (%)		Relative standard uncertainty (%)		Relative standard uncertainty (%)	
	Type A	Type B	Type A	Type B	Type A	Type B
Air kerma rate	0.16	0.35	0.16	0.35	0.16	0.35
Current measurement	0.35	0.05	0.32	0.05	0.42	0.05
Temperature	0.01	0.20	0.01	0.20	0.01	0.20
Pressure	0.01	0.10	0.01	0.10	0.01	0.10
Humidity		0.10		0.10		0.10
Quadratic sum	0.38	0.43	0.36	0.43	0.45	0.43
Combined standard uncertainty	0.58		0.56		0.62	

Table C6a. NMIJ/AIST uncertainty budget (CCRI radiation qualities)

Uncertainty associated with the standard

Source of component	Relative standard uncertainty (%)	
	Type A	Type B
Pysical constants		
Dry air density		0.01
W_{air}/e		0.15
$1-g_{air}$		0.01
Correction factors		
Scattered radiation		0.14
Fluoresence		
Electron loss		0.01
Ion recombination		0.02
Polarity		0.03
Air attenuation		0.15
Field distortion		0.005
Transmission through edges of diaphragm		0.01
Scattering from diahragm		0.01
Wall transmission		0.01
Humidity		0.03
Volume and current measurement		
Volume		0.12
Current measurement	0.05	0.04
Distance		0.06
Temperature		0.02
Pressure		0.05
Quadratic sum	0.05	0.30
Combined standard uncertainty	0.30	

Uncertainty associated with the calibration of the transfer chambers

Transfer chambers →	AE-1340C		NE 2536		Magna	
Source of component	Relative standard uncertainty (%)		Relative standard uncertainty (%)		Relative standard uncertainty (%)	
	Type A	Type B	Type A	Type B	Type A	Type B
Air kerma rate	0.05	0.30	0.05	0.30	0.05	0.30
Current measurement	0.10	0.04	0.10	0.04	0.10	0.04
Temperature		0.03		0.03		0.03
Pressure		0.05		0.05		0.05
Humidity		0.05		0.05		0.05
Distance		0.06		0.06		0.06
Field distortion		0.06		0.06		0.06
Scattered radiation		0.20		0.20		0.20
Quadratic sum	0.11	0.38	0.11	0.38	0.11	0.38
Combined standard uncertainty	0.40		0.40		0.40	

Table C6b. NMIJ/AIST uncertainty budget (ISO N-15)

Uncertainty associated with the standard

Source of component	Relative standard uncertainty (%)	
	Type A	Type B
Pysical constants		
Dry air density		0.01
W_{air}/e		0.15
$1\text{-}g_{air}$		0.01
Correction factors		
Scattered radiation		0.14
Fluoresence		
Electron loss		0.01
Ion recombination		0.02
Polarity		0.03
Air attenuation		0.15
Field distortion		0.01
Transmission through edges of diaphragm		0.01
Scattering from diahragm		0.01
Wall transmission		0.01
Humidity		0.03
Volume and current measurement		
Volume		0.12
Current measurement	0.10	0.04
Distance		0.06
Temperature		0.02
Pressure		0.05
Quadratic sum	0.10	0.30
Combined standard uncertainty	0.32	

Uncertainty associated with the calibration of the transfer chambers

Transfer chambers →	AE-1340C		NE 2536		Magna	
Source of component	Relative standard uncertainty (%)		Relative standard uncertainty (%)		Relative standard uncertainty (%)	
	Type A	Type B	Type A	Type B	Type A	Type B
Air kerma rate	0.10	0.30	0.10	0.30	0.10	0.30
Current measurement	0.40	0.04	0.40	0.04	0.10	0.04
Temperature		0.03		0.03		0.03
Pressure		0.05		0.05		0.05
Humidity		0.05		0.05		0.05
Distance		0.06		0.06		0.06
Field distortion		0.06		0.06		0.06
Scattered radiation		0.20		0.20		0.20
Quadratic sum	0.41	0.38	0.41	0.38	0.14	0.38
Combined standard uncertainty	0.56		0.56		0.41	

Table C6c. NMIJ/AIST uncertainty budget (ISO N-40)

Uncertainty associated with the standard

Source of component	Relative standard uncertainty (%)	
	Type A	Type B
Pysical constants		
Dry air density		0.01
W_{air}/e		0.15
$1\text{-}g_{air}$		0.01
Correction factors		
Scattered radiation		0.14
Fluoresence		
Electron loss		0.01
Ion recombination		0.02
Polarity		0.03
Air attenuation		0.15
Field distortion		0.01
Transmission through edges of diaphragm		0.01
Scattering from diahragm		0.01
Wall transmission		0.01
Humidity		0.03
Volume and current measurement		
Volume		0.12
Current measurement	0.10	0.04
Distance		0.06
Temperature		0.02
Pressure		0.05
Quadratic sum	0.10	0.30
Combined standard uncertainty	0.32	

Uncertainty associated with the calibration of the transfer chambers

Transfer chambers →	AE-1340C		NE 2536		Magna	
Source of component	Relative standard uncertainty (%)		Relative standard uncertainty (%)		Relative standard uncertainty (%)	
	Type A	Type B	Type A	Type B	Type A	Type B
Air kerma rate	0.10	0.30	0.10	0.30	0.10	0.30
Current measurement	0.50	0.04	0.40	0.04	0.10	0.04
Temperature		0.03		0.03		0.03
Pressure		0.05		0.05		0.05
Humidity		0.05		0.05		0.05
Distance		0.06		0.06		0.06
Field distortion		0.06		0.06		0.06
Scattered radiation		0.20		0.20		0.20
Quadratic sum	0.51	0.38	0.41	0.38	0.14	0.38
Combined standard uncertainty	0.64		0.56		0.41	

Table C7a. Nuc. Malaysia uncertainty budget (CCRI 10)

Uncertainty associated with the standard

Source of component	Relative standard uncertainty (%)	
	Type A	Type B
Air kerma rate		
N_k from PTB		0.39
Distance		0.06
Charge measurement	0.06	
Accuracy of charge		0.29
Temperature		0.07
Pressure		0.03
Quadratic sum	0.06	0.50
Combined standard uncertainty	0.50	

Uncertainty associated with the calibration of the transfer chambers

Transfer chambers →	AE-1340C		NE 2536		Magna	
Source of component	Relative standard uncertainty (%)		Relative standard uncertainty (%)		Relative standard uncertainty (%)	
	Type A	Type B	Type A	Type B	Type A	Type B
Air kerma rate	0.06	0.50	0.06	0.50	0.06	0.50
Charge measurement	0.06		0.04		0.01	
Temperature		0.07		0.07		0.07
Pressure		0.03		0.03		0.03
Distance		0.06		0.06		0.06
Accuracy of charge		0.29		0.29		0.29
Quadratic sum	0.08	0.58	0.07	0.58	0.06	0.58
Combined standard uncertainty	0.59		0.59		0.59	

Table C7b. Nuc. Malaysia uncertainty budget (CCRI 30)

Uncertainty associated with the standard

Source of component	Relative standard uncertainty (%)	
	Type A	Type B
Air kerma rate		
N_k from PTB		0.39
Distance		0.06
Charge measurement	0.01	
Accuracy of charge		0.29
Temperature		0.07
Pressure		0.03
Quadratic sum	0.01	0.50
Combined standard uncertainty	0.50	

Uncertainty associated with the calibration of the transfer chambers

Transfer chambers →	AE-1340C		NE 2536		Magna	
Source of component	Relative standard uncertainty (%)		Relative standard uncertainty (%)		Relative standard uncertainty (%)	
	Type A	Type B	Type A	Type B	Type A	Type B
Air kerma rate	0.01	0.50	0.01	0.50	0.01	0.50
Charge measurement	0.01		0.01		0.01	
Temperature		0.07		0.07		0.07
Pressure		0.03		0.03		0.03
Distance		0.06		0.06		0.06
Accuracy of charge		0.29		0.29		0.29
Quadratic sum	0.01	0.58	0.01	0.58	0.01	0.58
Combined standard uncertainty	0.58		0.58		0.58	

Table C7c. Nuc. Malaysia uncertainty budget (CCRI 25)

Uncertainty associated with the standard

Source of component	Relative standard uncertainty (%)	
	Type A	Type B
Air kerma rate		
N_k from PTB		0.39
Distance		0.06
Charge measurement	0.01	
Accuracy of charge		0.29
Temperature		0.07
Pressure		0.03
Quadratic sum	0.01	0.50
Combined standard uncertainty	0.50	

Uncertainty associated with the calibration of the transfer chambers

Transfer chambers →	AE-1340C		NE 2536		Magna	
Source of component	Relative standard uncertainty (%)		Relative standard uncertainty (%)		Relative standard uncertainty (%)	
	Type A	Type B	Type A	Type B	Type A	Type B
Air kerma rate	0.01	0.50	0.01	0.50	0.01	0.50
Charge measurement	0.02		0.04		0.01	
Temperature		0.07		0.07		0.07
Pressure		0.03		0.03		0.03
Distance		0.06		0.06		0.06
Accuracy of charge		0.29		0.29		0.29
Quadratic sum	0.02	0.58	0.04	0.58	0.01	0.58
Combined standard uncertainty	0.58		0.58		0.58	

Table C7d. Nucl. Malaysia uncertainty budget (CCRI 50b)

Uncertainty associated with the standard

Source of component	Relative standard uncertainty (%)	
	Type A	Type B
Air kerma rate		
N_k from PTB		0.39
Distance		0.06
Charge measurement	0.01	
Accuracy of charge		0.29
Temperature		0.07
Pressure		0.03
Quadratic sum	0.01	0.50
Combined standard uncertainty	0.50	

Uncertainty associated with the calibration of the transfer chambers

Transfer chambers →	AE-1340C		NE 2536		Magna	
Source of component	Relative standard uncertainty (%)		Relative standard uncertainty (%)		Relative standard uncertainty (%)	
	Type A	Type B	Type A	Type B	Type A	Type B
Air kerma rate	0.01	0.50	0.01	0.50	0.01	0.50
Charge measurement	0.01		0.02		0.01	
Temperature		0.07		0.07		0.07
Pressure		0.03		0.03		0.03
Distance		0.06		0.06		0.06
Accuracy of charge		0.29		0.29		0.29
Quadratic sum	0.01	0.58	0.02	0.58	0.01	0.58
Combined standard uncertainty	0.58		0.58		0.58	

Table C7e. Nuc. Malaysia uncertainty budget (CCRI 50a)

Uncertainty associated with the standard

Source of component	Relative standard uncertainty (%)	
	Type A	Type B
Air kerma rate		
N_k from PTB		0.39
Distance		0.06
Charge measurement	0.04	
Accuracy of charge		0.29
Temperature		0.07
Pressure		0.03
Quadratic sum	0.04	0.50
Combined standard uncertainty	0.50	

Uncertainty associated with the calibration of the transfer chambers

Transfer chambers →	AE-1340C		NE 2536		Magna	
Source of component	Relative standard uncertainty (%)		Relative standard uncertainty (%)		Relative standard uncertainty (%)	
	Type A	Type B	Type A	Type B	Type A	Type B
Air kerma rate	0.04	0.50	0.04	0.50	0.04	0.50
Charge measurement	0.04		0.11		0.01	
Temperature		0.07		0.07		0.07
Pressure		0.03		0.03		0.03
Distance		0.06		0.06		0.06
Accuracy of charge		0.29		0.29		0.29
Quadratic sum	0.06	0.58	0.12	0.58	0.04	0.58
Combined standard uncertainty	0.59		0.59		0.58	

Table C7f. Nuc. Malaysia uncertainty budget (ISO N-15)

Uncertainty associated with the standard

Source of component	Relative standard uncertainty (%)	
	Type A	Type B
Air kerma rate		
N_k from PTB		0.39
Distance		0.06
Charge measurement	0.03	
Accuracy of charge		0.29
Temperature		0.07
Pressure		0.03
Quadratic sum	0.03	0.50
Combined standard uncertainty	0.50	

Uncertainty associated with the calibration of the transfer chambers

Transfer chambers →	AE-1340C		NE 2536		Magna	
Source of component	Relative standard uncertainty (%)		Relative standard uncertainty (%)		Relative standard uncertainty (%)	
	Type A	Type B	Type A	Type B	Type A	Type B
Air kerma rate	0.03	0.50	0.03	0.50	0.03	0.50
Charge measurement	0.40		0.32		0.02	
Temperature		0.07		0.07		0.07
Pressure		0.03		0.03		0.03
Distance		0.06		0.06		0.06
Accuracy of charge		0.29		0.29		0.29
Quadratic sum	0.40	0.58	0.32	0.58	0.04	0.58
Combined standard uncertainty	0.71		0.67		0.58	

Table C7f. Nuc. Malaysia uncertainty budget (ISO N-40)

Uncertainty associated with the standard

Source of component	Relative standard uncertainty (%)	
	Type A	Type B
Air kerma rate		
N_k from PTB		0.39
Distance		0.06
Charge measurement	0.10	
Accuracy of charge		0.29
Temperature		0.07
Pressure		0.03
Quadratic sum	0.10	0.50
Combined standard uncertainty	0.51	

Uncertainty associated with the calibration of the transfer chambers

Transfer chambers →	AE-1340C		NE 2536		Magna	
Source of component	Relative standard uncertainty (%)		Relative standard uncertainty (%)		Relative standard uncertainty (%)	
	Type A	Type B	Type A	Type B	Type A	Type B
Air kerma rate	0.10	0.50	0.10	0.50	0.10	0.50
Charge measurement	0.57		1.04		0.05	
Temperature		0.07		0.07		0.07
Pressure		0.03		0.03		0.03
Distance		0.06		0.06		0.06
Accuracy of charge		0.29		0.29		0.29
Quadratic sum	0.58	0.58	1.04	0.58	0.11	0.58
Combined standard uncertainty	0.82		1.20		0.59	

Table C8a. NIM uncertainty budget (CCRI 10, 30, 25, 50b, 50a and ISO N-15)

Uncertainty associated with the standard

Source of component	Relative standard uncertainty (%)	
	Type A	Type B
Physical constants		
Dry air density		0.01
W_{air}/e		0.15
$1\text{-}g_{air}$		0.01
Correction factors		
Scattered radiation		0.10
Fluoresence		
Electron loss		0.01
Ion recombination	0.05	0.02
Polarity		0.05
Air attenuation	0.02	0.15
Field distortion		0.07
Transmission through edges of diaphragm		0.01
Scattering from diahragm		0.01
Wall transmission	0.05	
Humidity		0.03
Volume and current measurement		
Volume		0.01
Current measurement	0.05	0.05
Distance	0.02	0.02
Temperature		0.05
Pressure		0.04
Quadratic sum	0.09	0.27
Combined standard uncertainty	0.28	

Uncertainty associated with the calibration of the transfer chambers

Transfer chambers →	AE-1340C		NE 2536		Magna	
Source of component	Relative standard uncertainty (%)		Relative standard uncertainty (%)		Relative standard uncertainty (%)	
	Type A	Type B	Type A	Type B	Type A	Type B
Air kerma rate	0.09	0.27	0.09	0.27	0.09	0.27
Current measurement	0.10	0.05	0.10	0.05	0.10	0.05
Temperature		0.05		0.05		0.05
Pressure		0.04		0.04		0.04
Leakage		0.01		0.01		0.01
Distance	0.02	0.02	0.02	0.02	0.02	0.02
Stability		0.20		0.20		0.20
Quadratic sum	0.14	0.34	0.14	0.34	0.14	0.34
Combined standard uncertainty	0.37		0.37		0.37	

Table C8b. NIM uncertainty budget (ISO N-40)

Uncertainty associated with the standard

Source of component	Relative standard uncertainty (%)	
	Type A	Type B
Physical constants		
Dry air density		0.01
W_{air}/e		0.15
$1\text{-}g_{air}$		0.01
Correction factors		
Scattered radiation		0.10
Fluoresence		
Electron loss		0.01
Ion recombination	0.05	0.02
Polarity		0.05
Air attenuation	0.02	0.15
Field distortion		0.07
Transmission through edges of diaphragm		0.01
Scattering from diahragm		0.01
Wall transmission	0.05	
Humidity		0.03
Volume and current measurement		
Volume		0.01
Current measurement	0.05	0.05
Distance	0.02	0.02
Temperature		0.05
Pressure		0.04
Quadratic sum	0.09	0.27
Combined standard uncertainty	0.28	

Uncertainty associated with the calibration of the transfer chambers

Transfer chambers →	AE-1340C		NE 2536		Magna	
Source of component	Relative standard uncertainty (%)		Relative standard uncertainty (%)		Relative standard uncertainty (%)	
	Type A	Type B	Type A	Type B	Type A	Type B
Air kerma rate	0.09	0.27	0.09	0.27	0.09	0.27
Current measurement	0.30	0.05	0.30	0.05	0.10	0.05
Temperature		0.05		0.05		0.05
Pressure		0.04		0.04		0.04
Leakage		0.05		0.05		0.01
Distance	0.02	0.02	0.02	0.02	0.02	0.02
Stability		0.20		0.20		0.20
Quadratic sum	0.31	0.35	0.31	0.35	0.14	0.34
Combined standard uncertainty	0.47		0.47		0.37	

Table C9. OAP uncertainty budget

Uncertainty associated with the standard

Source of component	Relative standard uncertainty (%)	
	Type A	Type B
Air kerma rate		
N_k from NPL		0.90
Stability of calibration		0.20
Distance		0.10
Current measurement	1.50	
Electrometer resolution		0.02
Temperature		0.08
Pressure		0.06
Field inhomogeneity		0.20
X-ray output stability		0.20
Correction factor for the radiation quality		1.50
Quadratic sum	1.50	1.79
Combined standard uncertainty	2.33	

Uncertainty associated with the calibration of the transfer chambers

Transfer chambers →	AE-1340C		NE 2536		Magna	
Source of component	**Relative standard uncertainty (%)**		**Relative standard uncertainty (%)**		**Relative standard uncertainty (%)**	
	Type A	**Type B**	**Type A**	**Type B**	**Type A**	**Type B**
Air kerma rate	1.50	1.79	1.50	1.79	1.50	1.79
Current measurement	3.70		2.80		1.40	
Temperature		0.08		0.08		0.08
Pressure		0.06		0.06		0.06
Ion recombination		0.50		0.50		0.20
Leakage		0.10		0.10		0.10
Quadratic sum	3.99	1.86	3.18	1.86	2.05	1.81
Combined standard uncertainty	4.41		3.68		2.73	